The Thesis Committee for SHIRAZ GULRAIZ

Certifies that this is the approved version of the following thesis:

Existence of Plug Zones in Viscoplastic Fluid Flow and their Effect on Drilling Hydraulics in a Concentric Vertical Annulus

APPROVED BY

SUPERVISING COMMITTEE:

Kenneth E. Gray, Supervisor

Hugh C. Daigle

Existence of Plug Zones in Viscoplastic Fluid Flow and their Effect on Drilling Hydraulics in a Concentric Vertical Annulus

by

Shiraz Gulraiz

Thesis

Presented to the Faculty of the Graduate School of

The University of Texas at Austin

in Partial Fulfillment

of the Requirements

for the Degree of

Master of Science in Engineering

The University of Texas at Austin

December 2018

Dedication

To my parents, whatever I have achieved and will ever achieve is due to them,

to my younger sister and brother,

and to all the suns in Pakistan waiting to rise.

Acknowledgements

اول حمد ثنا الہی جو مالک ہر ہر دا

اس دا نام چتارن والا کسے میدان نہ ہردا

I would like to express my sincere gratitude to Dr. K.E Gray for giving me the opportunity to work as a part of Wider Windows consortium. I would also like to thank Dr. Daigle for his suggestions and guidance throughout my project and Dr. Bommer for having me as a Teaching Assistant.

No matter how hard I try, I will not be able to find words to thank my parents and my family. I think even the most eloquent of the speakers will never be able to find words to do so. All I can say is that this would not have been possible without my parents and my family.

Special thanks to my friends: Hasan Khan, Asad ul Haq, Saqib Khan, Mujtaba Khan, and Yusuf Nasir. I will always be indebted to you guys for your support and help.

Abstract

Existence of Plug Zones in Viscoplastic Fluid Flow and their Effect on Drilling Hydraulics in a Concentric Vertical Annulus

Shiraz Gulraiz, M.S.E

The University of Texas at Austin, 2018

Supervisor: Kenneth E. Gray

Drilling fluid, an example of a viscoplastic fluid, is a type of non-Newtonian fluid characterized by the existence of a threshold stress, called yield stress, that must be overcome for fluids to flow. Drilling fluid is conventionally modeled using power law parameters and yield stress. Yielded and unyielded zones that exist in viscoplastic flow due to varying shear rate profile in an annulus are not considered while modeling flow. This thesis investigates the factors affecting the existence of plug zones and the effect of plug zones on a fluid's cuttings carrying capacity and on annular pressure drop. A CFD model has been developed to carry out this investigation.

The first half of this thesis presents the effects of flow rate, yield stress and drillpipe rotation on the size of plug zone. The results show that plug size decreases with an increase in flow rate until a minimum limit is achieved. Plug is nonexistent when yield stress is small and its size increases and reaches a maximum limit as yield stress increases. Plug

zone ceases to exist when drillpipe is rotated at a speed greater than a critical speed. The critical speed is directly proportional to yield stress and inversely proportional to plug viscosity. Annular pressure drop increases with an increase in yield stress and plug viscosity though the rate of change of increase with respect to plug viscosity is comparatively small.

The second half of this thesis investigates the effects of plug zones on cuttings carrying capacity and on annular pressure drop in presence of drill cuttings. The effect of plug zone on cuttings carrying capacity increases as the size and/or density of the particle increases. It can be concluded that a fluid with higher plug zone viscosity has better cuttings carrying capacity. As yield stress increases and/or flow rate decreases, the impact of plug viscosity on annular pressure drop increases significantly. Therefore, for accurate prediction of annular pressure drop and cuttings transport, the size and viscosity of plug zone should be considered and incorporated in the rheological models.

Keywords: viscoplastic fluid; plug zones; concentric annulus; cuttings carrying capacity; annular pressure drop.

Table of Contents

List of Tables

List of Figures

CHAPTER 1: INTRODUCTION

1.1. Motivation

The main functions of a drilling fluid are to transport drill cuttings to the surface and ensure wellbore stability that is to prevent loss and kick scenarios. Although, much work has been done on cuttings transport and bottom hole pressure (BHP) prediction, the fine margins of drilling hydraulics are getting finer as the wells get deeper and more complex. In ultra-deep and extended reach wells, the ability to accurately predict the BHP and ensure proper hole cleaning is of paramount importance. The margin of error decreases further in wells with very narrow pore pressure and fracture pressure window. To ensure wellbore stability, it is imperative to consider the relationship between cuttings transport, BHP and the rheology of drilling fluid.

There is a significant change in drilling hydraulics once drill cuttings enter the annulus. Cuttings not only affect the BHP but also affect the rheology of drilling fluids. If not modeled accurately, the changes in the BHP and the rheology of drilling fluid due to the presence of cuttings can lead to several drilling problems such as high rotary torque, stuck pipe, formation breakdown and lost circulation.

1.2. Problem Statement

The rheology of drilling fluid lies at the core of drilling hydraulics. To accurately model velocity and pressure profiles, and concentration of drill cuttings in a wellbore, the rheological model used to describe shear stress vs. strain rate relationship of a drilling fluid is immensely significant. Drilling fluid is classified as a viscoplastic fluid. There are several models in the literature that describe stress-strain relationship of a viscoplastic fluid. Viscoplastic fluids are a type of non-Newtonian fluid characterized by the existence of a threshold stress, called yield stress, that must be overcome for the fluid to flow. After yield

stress value is exceeded, the fluid may exhibit Newtonian or shear thinning/thickening behavior. Drilling fluid is a typical example of a shear thinning fluid. Since shear rate is not the same everywhere in an annulus, this phenomenon results in a flow field that is comprised of two distinct regions: yielded zone and plug (unyielded) zone. An extensively used function to model drilling fluid was presented by Herschel and Bulkley (1926) and is given as:

$$\tau = \tau_y + K(\gamma)^n; \quad |\tau| > |\tau_y|$$
$$\tau = \tau_y; \quad |\tau| < |\tau_y| \tag{1.1}$$

where τ = shear stress, Υ= strain rate, τ_y = yield stress, and K and n are power law parameters.

In the literature related to drilling hydraulics, most of the studies model the rheology of the fluid using power law parameters (n and K) and yield stress. Some of the models used in literature are presented in the next chapter. To the author's knowledge, none of the studies found in literature consider plug zones that exist in viscoplastic fluid flow. This study investigates the factors affecting the existence and size of plug zones and the effect these plug zones have on a fluid's cuttings carrying capacity and on annular pressure drop.

1.3. Capabilities and Limitations

To avoid unintended generalizability, it is important to mention the capabilities and limitations of the computational fluid dynamics (CFD) model developed in this thesis.

1.3.1. Capabilities

- The model predicts BHP, velocity profiles and annular cuttings concentration.
- This is a 3-dimensional model. Most models in the literature are restricted to two dimensions which simplifies the problem at the cost of accuracy.
- This model predicts the size and shape of yielded and plug (unyielded) zones.
- A physics-based relative velocity model is employed to calculate the slip velocity between the solid and liquid phases.

1.3.2. Limitations

- The fluid flow is modeled as steady, incompressible, isothermal and laminar flow.
- The scope of this study is limited to concentric vertical annulus.
- The model considers monodispersed spherical particles.
- The model assumes that plug zone has a single viscosity value. This assumption is particularly useful when investigating the effects of plug zone.

CHAPTER 2: LITERATURE REVIEW

This chapter presents a review of the rheological models used to model the behavior of a viscoplastic fluid and the effects of the rheology of a fluid on cuttings transport and BHP.

2.1. Types of Fluids

Drilling fluids can be broadly divided into two categories, Newtonian and non-Newtonian fluids. The Newtonian model describes the simplest fluid flow behavior where the shear stress is directly proportional to shear rate under conditions of constant pressure and temperature. Viscosity, being the constant of proportionality, is defined as

$$\mu = \frac{\tau}{\gamma} \tag{2.1}$$

where μ = viscosity, τ = shear stress and Υ= strain rate.

Almost all drilling fluids are non-Newtonian in nature. The apparent viscosity of a non-Newtonian fluid is a function of space and depends on volumetric flow rate or pressure gradient. Non-Newtonian fluids can be further divided into shear thickening and shear thinning fluids.

2.1.1. Shear Thickening Fluids

The apparent viscosity of shear thickening fluids increases with increasing shear rate. Shear thickening fluids are also called dilatant fluids.

2.1.2. Shear Thinning Fluids

The apparent viscosity of shear thinning fluids decreases with increasing shear rate. Shear thinning fluids are also called pseudoplastic fluids. A widely used two parameters model that defines the apparent viscosity of a shear thinning fluid was presented by

Ostwald and De Waele (1923) and is generally known as power law model. The power law model is stated below.

$$\mu = K(\gamma)^{n-1} \tag{2.2}$$

where K and n are power law parameters.

2.1.3. Viscoplastic Fluids

Viscoplastic or yield stress fluids are a type of non-Newtonian fluids characterized by the existence of a threshold stress, called yield stress, that must be overcome for the fluids to flow. After yield stress value is exceeded, the fluid may exhibit Newtonian or shear thinning behavior. Two major types of viscoplastic fluids are stated below.

i. Bingham Plastic Fluids

Fluids that exhibit Newtonian behavior after yield stress is overcome are known as Bingham plastic fluids. The model was proposed by Bingham (1922) and is defined as

$$\begin{gathered} \tau = \tau_y + \mu_p \gamma; \quad |\tau| > |\tau_y| \\ \tau = \tau_y; \quad |\tau| < |\tau_y| \end{gathered} \tag{2.3}$$

where τ_y = yield stress and μ_p = plastic viscosity.

ii. Herschel Bulkley Fluids

Fluids that exhibit shear thinning behavior after yield stress is overcome are known as Herschel Bulkley fluids. The model was proposed by Herschel and Bulkley (1926) and is defined as

$$\tau = \tau_y + K(\gamma)^n; \quad |\tau| > |\tau_y| \tag{2.4}$$

$$\tau = \tau_y; \quad |\tau| < |\tau_y|$$

where K and n are power law parameters. Fig. 2.1 summarizes the behavior of different types of non-Newtonian fluids.

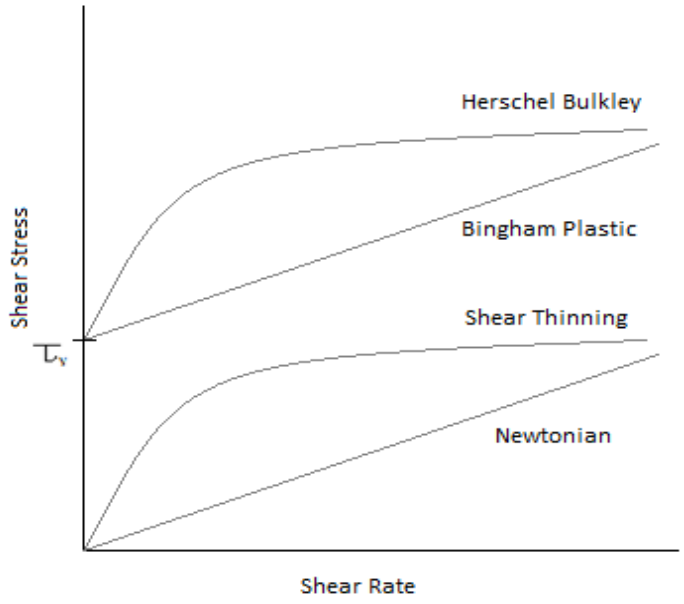

Figure 2.1: Shear stress vs. shear rate profile for different types of non-Newtonian fluids

2.2. Modeling Drilling Fluids

Bingham (1922), Herschel and Bulkley (1926) and Casson (1959) were some of the early authors who worked on viscoplastic fluids and presented mathematical functions to model shear stress vs. shear rate behavior of these fluids. Despite these publications, the literature on viscoplastic fluids remained limited until Bird et al. (1983) published an exhaustive review of the work done on viscoplastic fluids. This publication spurred a debate on the physical reality of viscoplastic fluids.

Barnes and Walters (1985) argued that yield stress does not exist, and it only defines a quantity that cannot be measured. Along the same lines, Wildemuth and Williams (1985) conducted an experimental study and showed that the concept of yield stress was just an instrumental error that occurred at low shear rates. On the other hand, O'Donovan and Tanner (1984) conducted an experiment where unyielded plug zones were replaced with solid bodies. The results of the setup with solid zones were compared with the case that had unyielded plug zones. Based on the similarity in stress and flow fields, it was concluded that plug zones do exist. Hartnett and Hu (1989), Astarita (1990) and Schurz (1990) also disputed the claims against the existence of yield stress and argued that yield stress is an engineering reality.

Drilling fluid is a typical example of a viscoplastic fluid. In the early literature pertaining of the petroleum industry, drilling fluid was modeled using the functions proposed by Ostwald and De Waele (1923), Bingham (1922), Herschel and Bulkley (1926) and Casson (1959). As drilling fluids got more complex, the above-mentioned models were found to be inadequate and therefore gave way to several other models. Besides the models mentioned above, the ones that found the most popularity in the literature are the Sisko model (Sisko, 1958) and the Robertson-Stiff model (Robertson et al., 1976). Khalil and Mohamed Jan (2012)

presented a summary of different models used to model the viscoplastic behavior of drilling fluids.

All the above-mentioned models fail to incorporate an extremely significant feature of viscoplastic fluids, plug zones. The fact that viscoplastic fluids do not flow unless the applied stress is greater than a threshold stress results in the existence of plug zones. Since shear rate is not the same everywhere in an annulus, this phenomenon produces a flow field that is comprised of two distinct regions: yielded zone and plug (unyielded) zone. Fig. 2.2 shows a schematic of plug zone in an annulus.

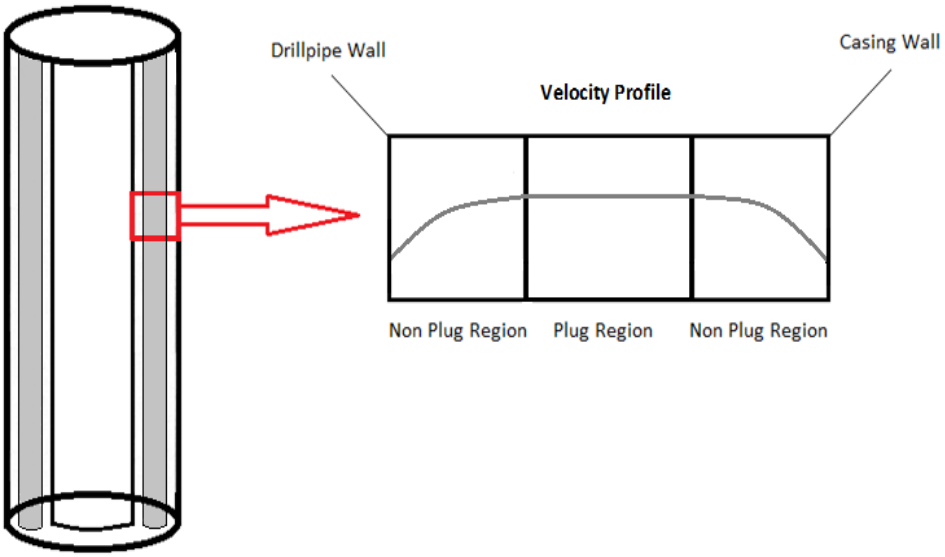

Figure 2.2: Plug zone in viscoplastic fluid flow

2.3. Modeling Plug Zones

Several studies have been devoted to the determination of the existence and the size of plug zones. Tanner and Milthorpe (1983) modeled the viscoplastic fluid as two Newtonian fluids having two viscosity values, one for the region where shear stress is below yield stress and second for the region where shear stress is greater than yield stress. Beris et al. (1985) used finite element methodology to model yielded and unyielded (plug) zones around a sphere falling in an infinite Bingham plastic fluid. Papanastasiou (1987) proposed a modified form of Herschel Bulkley function that predicted viscosity in both yielded and unyielded (plug) zones. The proposed function is given below.

$$\tau = (1 - e^{-\aleph\gamma})\tau_y + K(\gamma)^n \tag{2.5}$$

where ℵ is the regularizing parameter that controls the stress growth.

The model presented by Papanastasiou (1987) use a regularization parameter and therefore, the results are dependent on the value of the regularization parameter (Liu et al., 2002, Frigaard and Nouar, 2005, and de Souza Mendes et al., 2007). Apart from being dependent on the regularization parameter, the models presented by Papanastasiou (1987), Bingham (1922), Herschel and Bulkley (1926) and Casson (1959) fail to predict a finite viscosity when shear rate is zero. A modified version of the bi-viscosity model of Tanner and Milthorpe (1983) was used by O'Donovan and Tanner (1984), Beverly and Tanner (1989), and Beverly and Tanner (1992). The modified bi-viscosity model is given as:

$$\begin{aligned} \tau &= \tau_y + K(\gamma)^n \quad \text{if } \gamma > \frac{\tau_y}{\mu_{plug}} \\ \tau &= \mu_{plug}\gamma \quad \text{otherwise} \end{aligned} \tag{2.6}$$

where μ = viscosity, μ_{plug} = viscosity of the unyielded plug zone, τ_y = yield stress, Υ= strain rate and K and n are power law parameters.

de Souza Mendes and Dutra (2004) presented a comparison of several viscosity models including Papanastasiou's model and modified bi-viscosity function. de Souza Mendes and Dutra (2004) also proposed a modified version of Herschel Bulkley function to model the rheology of a viscoplastic fluid. This model removed the viscosity discontinuity at yield stress found in the previous models. Moreover, this model is independent of a regularization model and predicts the value of plug zone's viscosity. The viscosity function proposed by de Souza Mendes and Dutra (2004) is given as

$$\tau = [1 - e^{\frac{-\mu_{plug}(\gamma)}{\tau_y}}]\left[\tau_y + K(\gamma^n)\right] \tag{2.7}$$

where μ_{plug} is viscosity of plug zone.

2.4. Cuttings Carrying Capacity and Bottom Hole Pressure (BHP)

Cuttings transport has been extensively studied in the literature. This section does not include the studies conducted on eccentric and inclined annuli since the scope of this thesis is limited to concentric and vertical annuli.

The methodology adopted by the researchers can be broadly divided into two classes: the experimental approach in which empirical correlations were developed based on the observation or the analytical approach which employed the use of the more-fundamental mechanistic models. It is important to mention that these mechanistic models are not independent of empirical correlations either. These correlations have been mainly used to define relative velocity that is velocity of cuttings relative to drilling fluid, and to predict viscosity of a mixture of drilling fluid and suspended cuttings.

One of the earliest experimental investigation of cuttings transport was published by Sifferman et al. (1974) who conducted an experimental study on a 140-ft vertical flow system and used bentonite mud as drilling fluid. Sifferman et al. (1974) observed that annular velocity and drilling fluid's rheology were the most important factors that control cuttings transport. The results indicated that for a bentonite-based drilling fluid, annular velocities down to 50 ft/min were adequate. Higher velocities did not have a considerable effect on cuttings transport rather resulted in greater frictional losses. It was concluded that cuttings transport efficiency increased with increasing fluid viscosity and yield stress. The effect of yield stress was further explored by Buscall et al. (1982) who carried out an experimental investigation on a 80 mm long by 20 mm diameter cylindrical glass tube. Buscall et al. (1982) observed that a shear thinning fluid with higher yield stress improves particle suspension and therefore, concluded that viscosity cannot be used as a sole indicator of cuttings carrying capacity of a drilling fluid. This phenomenon was further investigated by Hussaini and Azar (1983) who performed experiments on a 50 ft long, and 5" by 1.2" diameter vertical annulus. Hussaini and Azar (1983) concluded that for efficient cuttings transport in a vertical well, fluid rheology plays an important role but only at low and medium velocities. Fig. 2.4 shows the relation between cuttings concentration and

annular velocities. Hussaini and Azar (1983) also observed that increasing yield strength, while keeping viscosity constant, improves hole cleaning. It was further noted that an increase in gel strength improved cutting carrying capacity but only at low and medium velocities. This led to a very important result; out of the two fluids having same yield stress, the one with higher gel strength has better cuttings carrying capacity. Therefore, this publication proposed that for an efficient hole cleaning fluid, gel strength along with yield point and viscosity needs to be properly defined.

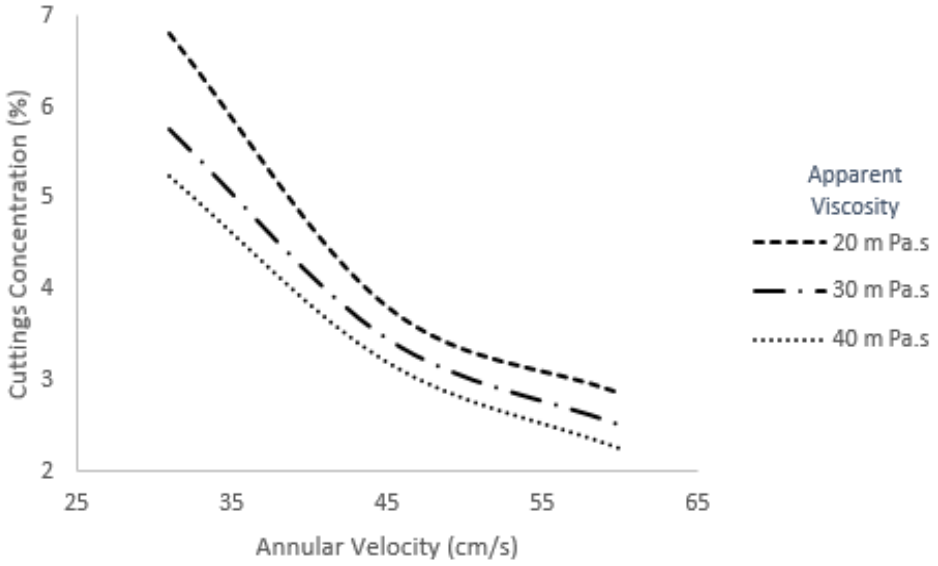

Figure 2.3: Cuttings concentration vs. annular velocity for gel/chemical system. Figure reconstructed from Hussaini and Azar (1983)

As pointed out by Sifferman et al. (1974), at high velocity values it is annular frictional pressure drop that is a concern instead of efficient cuttings transport. Therefore, ensuring efficient cuttings transport while keeping annular pressure drop within optimal bounds makes the rheology equally important even in a concentric vertical annulus. One of the first studies that predicted annular pressure drop and cuttings transport was published by Gavignet and Wick (1987) who formulated a simple computer model to carry out the above-mentioned tasks.

Advancements in computational technology motivated more and more authors to simulate complex equations instead of taking the experimental route. Clark and Bickham (1994) formulated a mechanistic model to predict minimum annular velocity required for efficient hole clearing. The model assumed that cuttings concentration was equal in plug and non-plug regions. It also did not define a way to calculate the diameter of plug zone. Clark and Bickham (1994) proposed that to keep cuttings concentration below 5% in a vertical well, annular velocity must exceed the velocity given below.

$$U_{mix} = \frac{0.0475 U_s}{0.05 - c_o} \tag{2.8}$$

$$U_s = U_{sa}\left[1 - \left(\frac{D_{plug}}{\sqrt{\left(D_h^2 - D_p^2\right)}}\right)^2\right] - U_{sp}\left[\frac{D_{plug}}{\sqrt{\left(D_h^2 - D_p^2\right)}}\right]^2 \tag{2.9}$$

$$c = \frac{Q_c}{Q_c + Q_m} \tag{2.10}$$

$$U_{sa} = \left[\frac{4dg(\rho_c - \rho)}{3\rho C_D}\right]^{\frac{1}{2}} (1 - c)^n \tag{2.11}$$

$$U_{sp} = U_{sp}^{*}\left(1 - \left[\frac{3\tau_y}{dg(\rho_c - \rho)}\right]^{0.94}\right) \tag{2.12}$$

$$U_{sp}^{*} = \left[\frac{4}{gC_D}\left(\frac{dg(\rho_c - \rho)}{3} - \pi\tau_y\right)\right]^{\frac{1}{2}} \tag{2.13}$$

$$\text{where } n = e^{0.0811y - 1.19},\ y = -\frac{sgn(x)}{(0.0001 + 0.865|x|^{-6})^{\frac{1}{6}}} \text{ and } x = 1.24\ln(Re) - 4.59 \tag{2.14}$$

where U_{mix} = mixture velocity, D_{plug} = diameter of plug zone, D_h = wellbore diameter, D_p = drillpipe diameter, ρ = density of drilling fluid, ρ_c = density of drill cuttings, Q_c = volumetric flow rate of cuttings, Q_m = volumetric flow rate of drilling fluid and Re = Reynold's number.

Özbelge and Beyaz (2001) conducted an experimental study to investigate cuttings profile and annular pressure drop in an annulus. The experiments were conducted on 500 cm long, 2.5 by 12.5 cm diameter annulus. Özbelge and Beyaz (2001) reported that annular pressure drop increased with increasing particle size and the concentration of the solid particles was higher near the outer wall compared to the inner wall. This was followed by another experimental investigation carried out by Han et al. (2010) who used a 1.8 m long and 30 by 44 mm diameter annulus to conduct the experiments. Han et al. (2010) compared two fluids that had almost equal viscosities but different densities and observed that the one with higher density had better cuttings carrying efficiency but also caused higher annular pressure drop. Han et al. (2010) also noted that the rotation of drillpipe improves cuttings transport and increases annular pressure drop. Contradictory results have been presented in the literature regarding the effect of drillpipe rotation on annular pressure drop. Several authors have reported a reduction in pressure drop due to drillpipe rotation while others have reported a significant increase in the pressure drop due to drillpipe rotation.

Refer to Ahmed and Miska (2008) for a summary of the conflicting results presented in the literature.

Al-Kayiem et al. (2010) formulated a mechanistic model of cutting transport process in the annulus and used CFD methodology to solve it. The simulated annular velocity profile was observed to be flat at around the center of the annulus. This study also confirmed that cuttings transport efficiency increases as particles get smaller in size. To investigate the effect of cutting shape on hole cleaning efficiency, particles with different shape factors were considered. The shape factor is simply a measure of the sphericity of a cutting particle. A cubic shape has a shape factor of 0.85, while the sphere has a shape factor of 1. A slight improvement in cuttings transport efficiency was noted as the shape factor increased.

Most studies focus on the effects of fluid's rheology on cuttings transport. There are very few publications that investigated the effect of cuttings on fluid's rheology. One of such investigation was carried out by Adekomaya et al. (2011) who experimentally studied the effects of drill cuttings on oil-based mud. Adekomaya et al. (2011) observed the plastic viscosity increased gradually up to cuttings concentration of 5% and then took a sharp increase from 6%. The sharp increase in plastic viscosity was attributed to the increase in surface area of the particles. The fluid loss also increased sharply above 5% cuttings concentration. The results also showed that an increase in cuttings concentration causes a corresponding increase in yield point, apparent viscosity, electrical stability, mud weight and gel strength.

Ofei et al. (2015) presented a cuttings-liquid frictional pressure drop model for narrow annuli with drillpipe rotation using Dimensional Analysis. The constants from the Dimensional Analysis were found using a simulation study. The parameters that affect annular pressure drop were listed as annular geometry, cuttings concentration, drillpipe rotation, axial and tangential fluid velocities, fluid density and viscosity, inclination and cuttings density and size. The effect of eccentricity was not considered. The annular pressure drop model presented by Ofei et al. (2015) is given below.

$$\frac{\Delta P}{\Delta L} = 0.255[(10^5 \Pi_1^{-2.021})(\Pi_2^{-2.021})(\Pi_3^{-1.51})(\Pi_4^{1.105})(\Pi_5^{0.967})(\Pi_6^{-1.118})] \quad (2.15)$$

where

$$\Pi_1 = D_i/D_o \quad (2.16)$$

$$\Pi_2 = \alpha \quad (2.17)$$

$$\Pi_3 = (\rho_m)(v_a)(D_o - D_i)/\mu_m \quad (2.18)$$

$$\Pi_4 = (\rho_m)(v_\Omega)(D_o - D_i)/\mu_m \quad (2.19)$$

$$\Pi_5 = v_a^2/g(D_o - D_i) \quad (2.20)$$

$$\Pi_6 = \Omega(D_o - D_i)/v_a \quad (2.21)$$

where g = gravitational acceleration, Ω = drillpipe rotation, D_i = drillpipe diameter, D_o = hole diameter, α = cuttings concentration, ρ_m = mixture density, μ_m = mixture viscosity, v_a = axial fluid velocity and v_Ω = tangential fluid velocity.

The model presented above is valid for drillpipe rotation ranging from 80 to 120 rpm. Cuttings size and wellbore inclination were kept constant. The expressions for axial and tangential velocities are given below.

$$v_a = \frac{4Q}{\pi(D_o - D_o)} \quad (2.22)$$

$$v_{\Omega} = \frac{(\frac{D_i}{D_o})^2 D_o \Omega}{\left[\left(\frac{D_i}{D_o}\right)^2 - 1\right](D_o^2 - D_i^2)}\left[\left(\frac{D_o^3 - D_i^2}{3D_o}\right) - (D_o^2 - D_o D_i)\right] \quad (2.23)$$

where Q = flow rate of drilling fluid.

A recent publication by Mohammadzadeh et al. (2016) examined the effects of fluid viscosity on particle transport capacity of fluid by considering various parameters such as density, diameter, shape and initial particle concentration. In this study, two phase flow with non-Newtonian fluid with yield stress as the base fluid was simulated using CFD technique. Mohammadzadeh et al. (2016) observed that cuttings concentration is at the lowest value at the center of the annulus and at maximum near the walls.

The effects of density, viscosity, yield stress and gel strength on cuttings transport and BHP are well established in the literature. Although plug zone is a well-researched topic in the field of non-Newtonian fluid mechanics, it has not been touched upon in the literature related to petroleum industry. The aim of this thesis is to have a deeper look into the rheology of a viscoplastic fluid and its effect on cuttings transport and BHP. This thesis investigates the effect of plug zones on cuttings transport and BHP in a concentric vertical annulus. The following chapter presents the methodology used to carry out the above-mentioned investigation.

CHAPTER 3: METHODOLOGY

This chapter presents the methodology employed to create a CFD based model to simulate the flow of viscoplastic fluids in annuli.

3.1. Multiphase Flow

The flow of a mixture that contains more than one phase is defined as a multiphase system. Annular flow consisting of drilling fluid and rock cuttings is a classic example of a multiphase system. There are two major approaches found in literature for the modeling of a multiphase flow.

3.1.1. Two Phase Model

The two phase model separately considers the complete continuity and momentum balances of each phase. These two sets of equations are coupled by momentum interactions.

3.1.2. Mixture (Diffusion) Model

The mixture (diffusion) model regards the whole particle-fluid combination as a single flowing continuum, the mixture fluid. This mixture has "effective" macroscopic properties e.g. viscosity. Apart from continuity and momentum balances for the mixture, the continuity equation of the dispersed component is incorporated in the formulation.

Multiphase flows are very complex, a single model applicable to all multiphase situations does not exist. Multiphase models are generally formulated for specific type of problem, both approaches (two phase and mixture) are reliant on some heuristic and/or semi-empirical correlations for closure equations**.** This study uses the mixture approach to model the annular flow since the mixture approach is computationally more efficient (takes less time) than the two-phase approach.

3.2. Model Formulation

This section presents the equations, rheological model and the meshing resolution used in this model. Fluid flow is modeled as steady, incompressible, isothermal and laminar flow. Apart from the continuity and mixture equations, the model requires closure relations for relative velocity and mixture viscosity.

3.2.1. Continuity equation for mixture

The continuity equation for a mixture is given as:

$$\frac{\partial \rho_m}{\partial t} + \nabla . (\rho_m v_m) = 0 \tag{3.1}$$

Mixture velocity, v_m, represents the velocity of the mass center. Mixture density, ρ_m, is defined as:

$$\rho_m = \alpha_D \rho_m + (1 - \alpha_D)\rho_c \rho_m = \alpha_D \rho_m + (1 - \alpha_D)\rho_c \tag{3.2}$$

where α_D is the volume fraction of dispersed particles and ρ_c is the density of the continuous phase.

3.2.2. Momentum Equation for mixture

The momentum equation for a mixture is given as:

$$\rho_m \left[\frac{Dv_m}{Dt} + 2\Omega \times v_m\right] = -\nabla P_m + \rho_m F + \nabla . \tau_G + \nabla . \tau_{Diff} + M_m \tag{3.3}$$

where D/Dt = material derivative, Ω = angular velocity, P_m = mixture pressure, F = body force per unit mass, τ_G = generalized stress, τ_{Diff} = diffusion stress and M_m = momentum transfer to the mixture due to surface tension.

In the equation above, pressure of both phases (solid and liquid) is taken to be equal to mixture pressure, P_m. The LHS of the equation has advection and Coriolis acceleration terms, while the RHS has the pressure, body force per unit mass, generalized stress and diffusion stress. To complete the system, constitutive equations for relative velocity, generalize stress and diffusion stress are required.

The body force per unit mass defined by Ungarish (1993) is given as

$$F = g - \Omega \times (\Omega \times \hat{r}) \tag{3.4}$$

where g is gravitational acceleration and $\hat{r}$ is the distance vector from the axis of rotation.

The generalized stress was defined by Hirsch (1988) and is given as

$$\nabla . \tau_G = \mu_{mix} \left[\nabla^2 v_m + \frac{1}{3} \nabla (\nabla . v_m) \right] \tag{3.5}$$

The deviatoric part of stress field is give as:

$$\begin{gathered} \tau = \tau_y + K|D|^n \quad \text{if } |D| > \frac{\tau_y}{\mu_{plug}} \\ \tau \leq \tau_y \quad \text{if } |D| = 0 \end{gathered} \tag{3.6}$$

The diffusion stress was defined by Verloop (1995) and is given as

$$\nabla . \tau_{Diff} = -\nabla . \alpha(1 - \alpha) \frac{\rho_c \rho_D}{\rho_m} v_R v_R \tag{3.7}$$

In eq. 3.7, v_R is relative velocity. According to Ungarish (1993), M_m, the mixture momentum source is ignored in practical applications.

3.2.3. Continuity equation for dispersed phase

The continuity equation for the dispersed phase, rock cuttings in this case, is given as

$$\frac{\partial \alpha_D}{\partial t} + \nabla.(\alpha_D v_m) = -\nabla.\left[\alpha_D\left(1 - \frac{\alpha_D \rho_D}{\rho_m}\right) v_R\right] \tag{3.8}$$

3.2.4. Relative Velocity

The closure equation for relative velocity is one of the most critical components of multiphase models. Chapter 2 states some closure equations used in the literature. The closure equation used in this study is formulated using the method used by Manninen et al. (1998).

The momentum equation for the dispersed phase can be written by using eq. 3.3 as

$$\begin{aligned} \alpha_D \rho_D \frac{\partial v_D}{\partial t} + \alpha_D \rho_D (v_D.\nabla) v_D + \alpha_D \rho_D (2\Omega \times v_D) \\ = -\alpha_D \nabla P_D + \alpha_D \rho_D F_D + \nabla.[\alpha_D \tau_{GD}] + M_D \end{aligned} \tag{3.9}$$

where F_D is body force per unit mass of the dispersed particle, τ_{GD} is generalized stress of the dispersed particle and M_D is the momentum transfer to the mixture due to surface tension.

The corresponding momentum equation for the mixture can be written as

$$\begin{aligned} \frac{\partial \rho_m v_m}{\partial t} + \rho_m (v_m.\nabla) v_m + \rho_m (2\Omega \times v_m) \\ = -\nabla P_m + \rho_m F_m + \nabla.(\tau_{Gm} + \tau_{Dm}) \end{aligned} \tag{3.10}$$

where F_m is body force per unit mass of the mixture, τ_{Gm} is generalized stress of the mixture, and τ_{Dm} is diffusion stress of the mixture.

In the equation above, surface tension forces are assumed to be negligible and hence, $M_m = 0$.

Setting $P = P_D = P_m$ yields

$$\begin{aligned} M_D = \alpha_D \left[\rho_D \frac{\partial v_R}{\partial t} + (\rho_D - \rho_m)\frac{\partial v_m}{\partial t}\right] + \alpha_D \rho_D (v_D . \nabla) v_D \\ - \alpha_D \rho_m (v_m . \nabla) v_m - \alpha_D \rho_D F_D + \alpha_D \rho_m F_m - \nabla . [\alpha_D (\tau_{GD})] \\ + \nabla . [\alpha_D (\tau_{Gm})] + \nabla . \tau_{Dm} + \alpha_D \rho_D (2\Omega \times v_D) \\ - \alpha_D \rho_m (2\Omega \times v_m) \end{aligned} \quad (3.11)$$

Setting $F_m = F_D$ in equation 3.11 can be written as

$$\begin{aligned} M_D = \alpha_D \left[\rho_D \frac{\partial v_R}{\partial t} + (\rho_D - \rho_m)\frac{\partial v_m}{\partial t}\right] + \alpha_D \rho_D (v_D . \nabla) v_D \\ - \alpha_D \rho_m (v_m . \nabla) v_m - -\nabla . [\alpha_D (\tau_{GD})] + \nabla . [\alpha_D (\tau_{Gm})] \\ + \nabla . \tau_{Dm} + \alpha_D \rho_D (2\Omega \times v_D) - - \alpha_D \rho_m (2\Omega \times v_m) \\ - \alpha_D (\rho_D - \rho_m) F \end{aligned} \quad (3.12)$$

To simplify eq. 3.12, it is assumed that the time derivative of $v_R = 0$ since v_R is usually a small value. The second term on the RHS of eq. 3.12 is approximated as

$$(v_D . \nabla) v_D \approx (v_m . \nabla) v_m \quad (3.13)$$

Neglecting the stresses, since they are small compared to the leading terms, yields

$$M_D = \alpha_D(\rho_D - \rho_m)[\frac{\partial v_m}{\partial t} + (v_m.\nabla)v_m] + \alpha_D\rho_D(2\Omega \times v_D) - \alpha_D\rho_m(2\Omega \times v_m) - \alpha_D(\rho_D - \rho_m)F \quad (3.14)$$

The drag force, F_{Drag}, can be written as

$$F_{Drag} = -\left[\frac{3}{4}\frac{\alpha_D\rho_C C_D}{d_p}\right]v_R^2 \quad (3.15)$$

Equating eq. 3.14 with 3.15 and making v_R the subject of the equation results in

$$v_R^2 = -\left[\frac{4}{3}\frac{d_p}{\rho_C C_D}\right]\{(\rho_D - \rho_m)[\frac{\partial v_m}{\partial t} + (v_m.\nabla)v_m] + \rho_D(2\Omega \times v_D) - \rho_m(2\Omega \times v_m) - \alpha_D(\rho_D - \rho_m)F\} \quad (3.16)$$

3.2.5. Viscosity of the Continuous phase

This study uses modified bi-viscosity function to model the flow of a viscoplastic fluid. The modified bi-viscosity function is easy to implement in numerical solutions and does not rely on a regularization parameter. Another advantage of this model is that it allows a single viscosity value to be assigned for plug zone which is useful when investigating the effects of plug viscosity. The viscosity function consists of two expressions that are applicable for different ranges of yield stress and is defined as

$$\tau = \tau_y + K(\gamma)^n \quad \text{if } \gamma > \frac{\tau_y}{\mu_{plug}}$$
$$\tau = \mu_{plug}\gamma \quad \text{otherwise} \quad (3.17)$$

where μ = viscosity, μ_{plug} = viscosity of the unyielded plug zone, τ_y = yield stress, Υ= strain rate and K and n are power law parameters.

Modified bi-viscosity function assumes that fluid has a very high constant viscosity when shear rate is less than τ_y/μ_{plug}. Once the shear rate is above this value, fluid behavior is predicted by Herschel Bulkley model. Fig. 3.1 shows the behavior of modified bi-viscosity model.

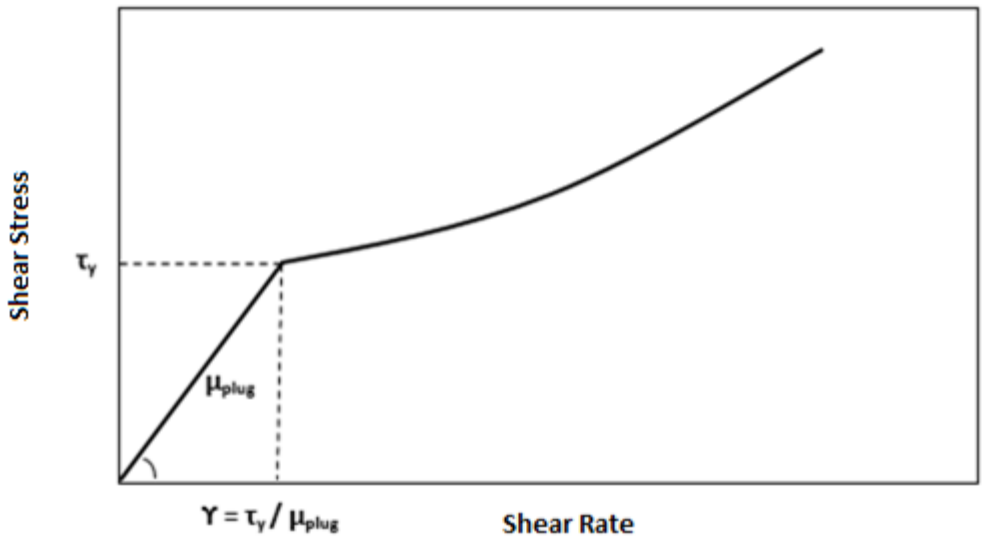

Figure 3.1: Shear stress vs. shear rate profile as predicted by the modified bi-viscosity function

3.2.6. Drag Coefficient

An expression for drag coefficient, proposed by Schiller and Naumann, (1935), is often used in the literature and is given below.

$$C_{Drag} = \left[\frac{24}{N_{RE}}(1 + 0.1N_{RE}^{0.75})\right] \tag{3.18}$$

where N_{RE} is Reynold's number and is defined as

$$N_{RE} = \frac{d_p \rho_c |v_R|}{\mu_c} \tag{3.19}$$

and v_R is relative velocity.

The expression proposed by Schiller and Naumann (1935) applies to single particle in a fluid. In a suspension, the influence of the distortion of flow field caused by the presence of dispersed particles needs to be considered. The resistance experienced by a particle in a suspension increases as the volume of solids increase. Ishii and Mishima (1984) proposed an expression for drag coefficient in a suspension. Drag coefficient is given as

$$C_{Drag} = \frac{24}{N_{RE}}\left[1 + 0.1 N_{RE}^{0.75}\right] \quad \text{if } N_{RE} < 1000$$

$$C_{Drag} = 0.45 \left\{ \frac{1 + 17.67\left[f(\alpha_D)^{\frac{6}{7}}\right]}{18.67[f(\alpha_D)]} \right\} \quad \text{if } N_{RE} > 1000 \tag{3.20}$$

where

$$f(\alpha_D) = \sqrt{(1 - \alpha_D)}\left(\frac{\mu_c}{\mu_m}\right)$$

$$N_{RE} = \frac{d_p \rho_c |V_R|}{\mu_m} \tag{3.21}$$

Eq. 3.23 shows that drag coefficient, C_{Drag}, is a function of relative velocity. It is worth mentioning here that relative velocity, eq. 3.16, is also a function of drag coefficient, C_{Drag}. Therefore, the equations for v_R and C_{Drag} needs to be solved iteratively. Also, note that in eq. 3.21, mixture viscosity is used instead of the viscosity of the continuous phase. The function used for mixture viscosity is given next.

3.2.7. Mixture Viscosity

The rheological properties of drilling fluid change in the presence of solid particles (rock cuttings). The global resistance to flow increases as drilling fluid now encounters additional boundaries of solid particles. Thus, viscosity of the mixture, drilling fluid and solid particles, is larger than that of particle-free drilling fluid.

There are several models in the literature that predict viscosity of a mixture. This study uses the semi-empirical correlation proposed by Ishii and Zuber (1979). For rigid spherical particles, the formula is given as follow:

$$\mu_m = \mu_c(1 - \alpha_D)^{-3.1} \tag{3.22}$$

3.3. CFD Simulation

To solve the multiphase flow model, an open source computational fluid dynamics (CFD) software is used in this study. CFD software use discretization procedures to solve a set of coupled differential equation. With the increase of computational power, CFD models have substituted experimental studies and empirical correlations, providing a cheaper way of solving complex engineering problems.

OpenFOAM is an open-source CFD software written in C++ and is available free of cost. OpenFOAM allows the user to customize the code and create individualized solutions for a specific model. OpenFOAM uses finite volume methodology (FVM) to discretize and solve coupled differential equations. The discretization procedure starts by defining the 3D workspace, called a mesh. In a mesh, the workspace is divided into small volumes. The next step is to define the initial and boundary conditions. The FVM approach applies the set of equations to the center of each control volume defined in the mesh. Difference interpolation schemes are the used to calculate the values at the faces of the control volumes.

Defining an equation in an OpenFOAM solver is relatively simple. The syntax of an equation in the code is very similar to the mathematical form of an equation. For example, the following equation:

$$\frac{\partial \rho v}{\partial t} + \nabla . \rho v - \nabla . \mu \nabla v = -\nabla P \tag{3.23}$$

is written in the code as

```
solve
(
    fvm::ddt(rho,v)
    + fvm::div(rho,v)
    – fvm::laplacian(mu,v)
    ==
    fvc::grad(p)
);
```

3.4. Meshing

Mesh resolution can have a significant effect on the results of a numerical simulation. Different mesh resolutions were employed for this study and the results were compared with the experimental data. The meshing resolution that showed the best agreement with the experimental data was chosen. There is no experimental work in literature to this author's knowledge that measures the annular pressure drop while varying the viscosity of plug zone as well. Due to this reason, fluid modeled by Herschel Bulkley model was used to compare the results and come up with the best mesh resolution. Chapter 4 presents the comparison with the experimental data.

3.5. Time Step

In CFD simulations, generally it is recommended that the Courant number should always remain less than 1 for the simulation to be stable and converging. In one dimension, the Courant number, C_o, is defined as

$$\mathrm{Co} = \frac{\Delta t|v|}{\Delta x} \tag{3.24}$$

where Δt is the time step, v is the velocity of the fluid and Δx is the width of the mesh cell in the direction of the velocity, v.

Eq. 3.24 shows that the Courant number is directly proportional to the time step and inversely proportional to the cell width. This means that keeping Courant number less than 1 is a tradeoff between simulation time and meshing resolution. In CFD simulation, decreasing the meshing resolution generally leads to a decrease in the accuracy of the model but according to eq. 3.24, a smaller mesh cell will require a smaller time step, therefore increasing the total simulation time. Eq. 3.24 also shows that the Courant number is directly proportional to the velocity though the meshing cell. Therefore, a higher flow rate will require a smaller time step or a bigger cell for the Courant number to remain below 1.

CHAPTER 4: MODEL VALIDATION

This chapter presents the results of this study. The simulation results are compared with the experimental data presented in the literature.

4.1. Case 1: Without Cuttings Loading

The simulation results were compared with the experimental study conducted by Ahmed and Miska (2008). The effects of drillpipe rotation on annular pressure drop were experimentally investigated. These experiments were carried out using a non-Newtonian fluid, the rheological parameters of the fluid are presented in Table 4.1. This study was conducted on a 3 m long, 1.5-inch x 1-inch annulus.

Table 4.1: Rheological parameters in Ahmed and Miska, (2008)

τ_y (Pa)	K (Pa s)	n
0	0.83	0.56

Fig. 4.1 compares simulated pressure drop with experimental data and the values predicted by a mathematical model employed by Ahmed and Miska (2008). The CFD model presented in this study under predicts the values at lower velocities and over predicts at higher velocities. Polymeric shear thinning solutions exhibit Newtonian behavior at very low and very high shear rates and power law behavior in between extreme shear rates. This implies that viscosity of fluid is approximately constant at extreme shear rates and decreases non-linearly with increasing shear rates for the region between the two Newtonian extremes. Fig. 4.2 shows the full spectrum of flow behavior in a polymeric shear thinning fluid. In the figure below, simulated data refers to the values predicted by

the CFD model developed in this study and the predicted data refers to the values that were obtained from a mathematical model employed by Ahmed and Miska (2008).

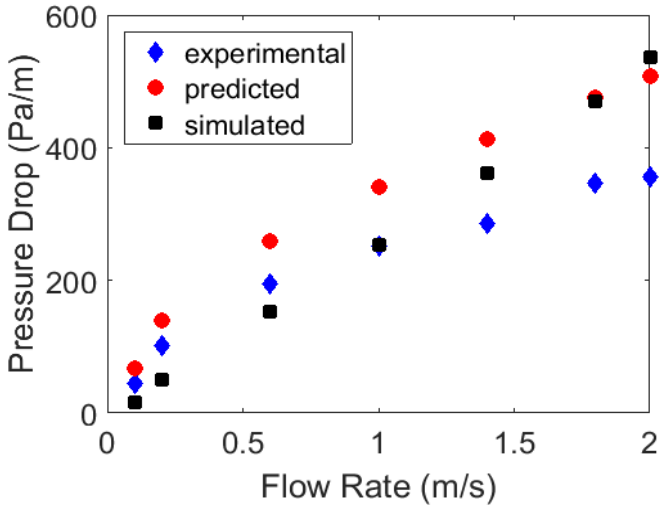

Figure 4.1: Experimental, simulated and predicted pressure drop

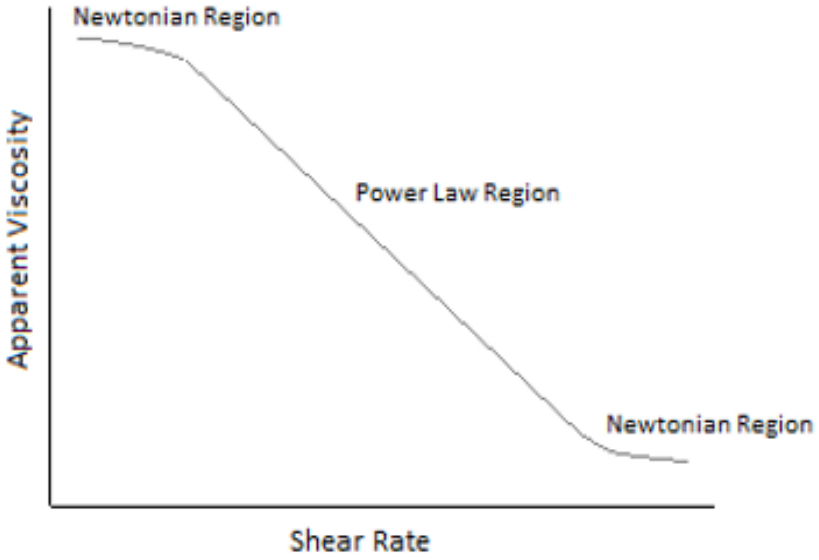

Figure 4.2: Complete viscosity profile of a polymeric shear thinning fluid

The viscosity model used in this study requires the complete viscosity spectrum. A possible reason for the discrepancies between the simulated and experimental results is the unavailability of the required viscosity data in Ahmed and Miska (2008). This study uses an extrapolated value as viscosity at zero shear rate. The extrapolated value is surely greater than the actual value which is not known in this case. Another reason for the differences in the results could be the inability to place drillpipe in perfectly concentric configuration in the experimental setup. In an eccentric annulus, the dominant flow phenomenon is the inertial effect that causes the pressure drop to increase. The effect of eccentricity in more pronounced in annuli with high diameter ratio. Fig. 4.3 compare the pressure drop at different velocities at different rotational speeds.

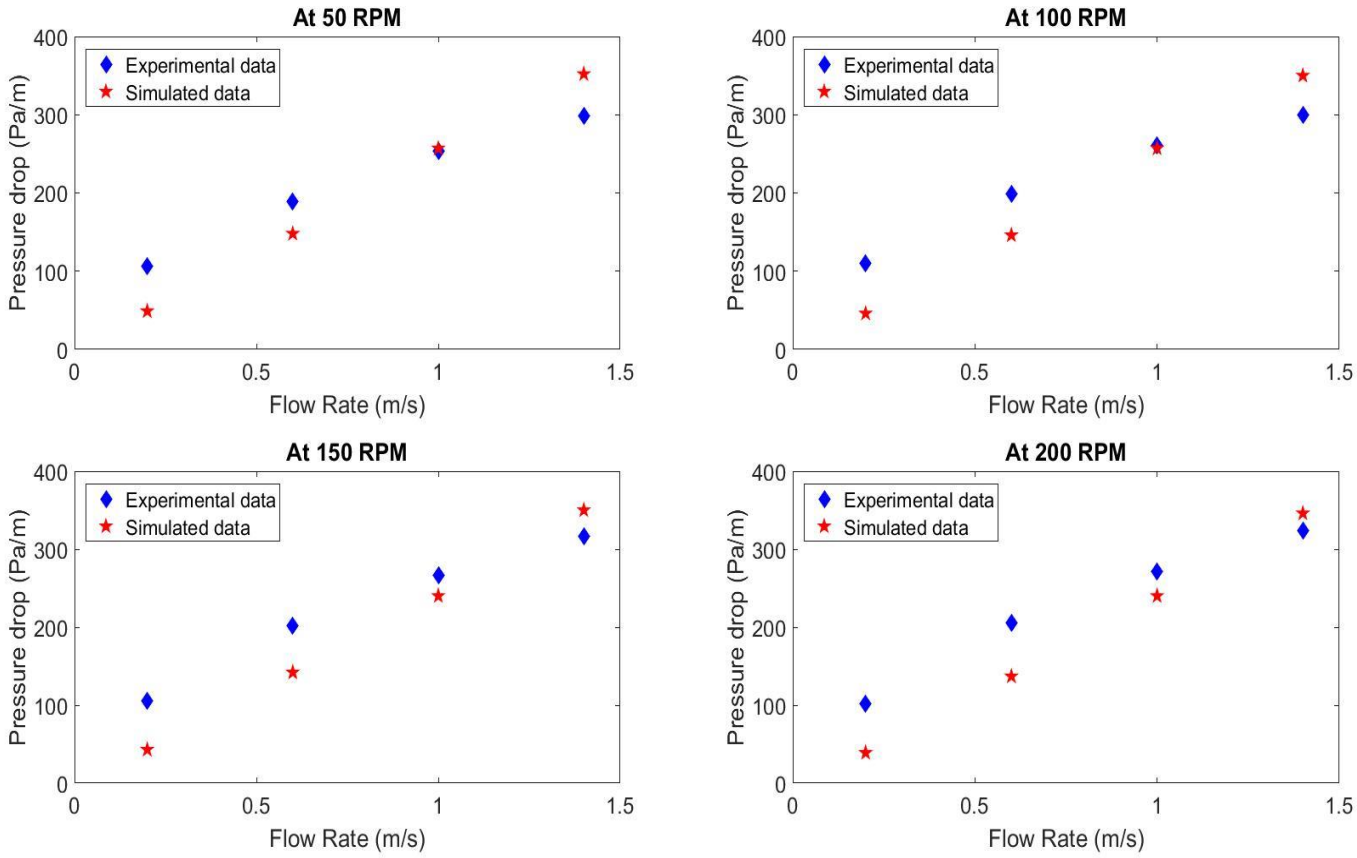

Figure 4.3: Pressure drop vs. flow rate at different rotational speeds.

As mentioned in Chapter 2, annular frictional pressure drop decreases with an increase in drillpipe rotation speed. This happens because in a perfectly concentric annulus, shear thinning is the dominant flow phenomenon and the cause of the reduction in the pressure drop. Fig. 4.4 shows the change in the pressure drop against speed of rotation for different flow rates. Drillpipe rotation causes a reduction in the pressure drop in a concentric annulus but this effect decreases as flow rate increases. This happens because the rate of change of apparent viscosity with shear rate decreases as the shear rate increases.

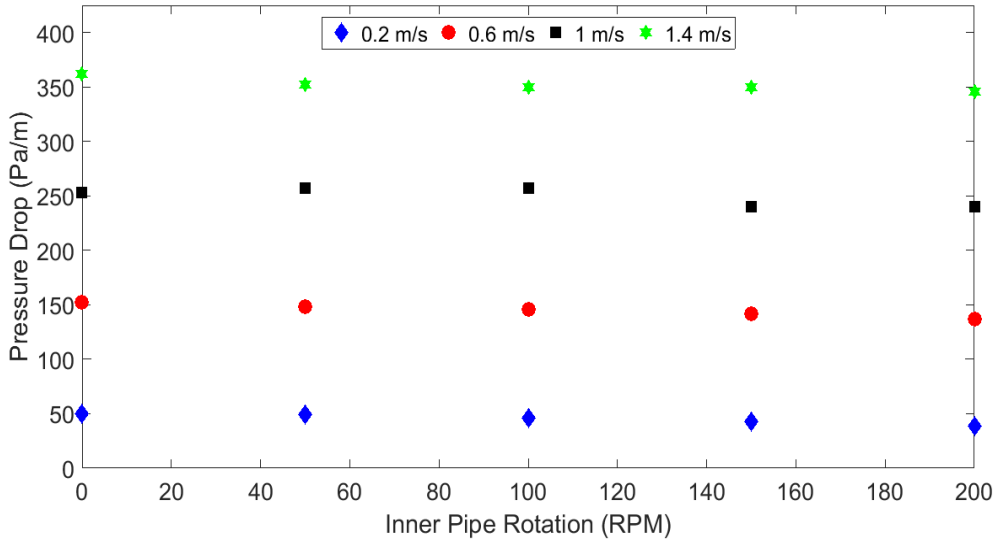

Figure 4.4: Pressure drop vs. rotational speed at different flow rates.

4.2. Case 2: With Cuttings Loading

The simulation results were compared with the experimental study conducted by Han et al. (2010) who investigated the hydraulic transport of sand particles in a vertical annulus with drillpipe rotation. The experiments were carried out on a 30-mm x 40-mm, 1.8 m long annulus. Bentonite solution was used as drilling fluid. Fig. 4.5 to 4.8 compare the simulated and experimental pressure drop values. Table 4.2 presents the rheological parameters of drilling fluid used by Han et al. (2010) As in the previous case, the lowest viscosity of the fluid is taken to be the viscosity of water. The experimental values (pressure and flow rate) were not explicitly stated in Han et al. (2010), and therefore had to be read off from the graphs presented in the study.

Table 4.2: Rheological parameters in Han et al., 2010.

Viscosity at 0 RPM (cp)	Viscosity at 200 RPM (cp)	N	Density (kg/m^3)
40.6	35.9	0.73	1041.1

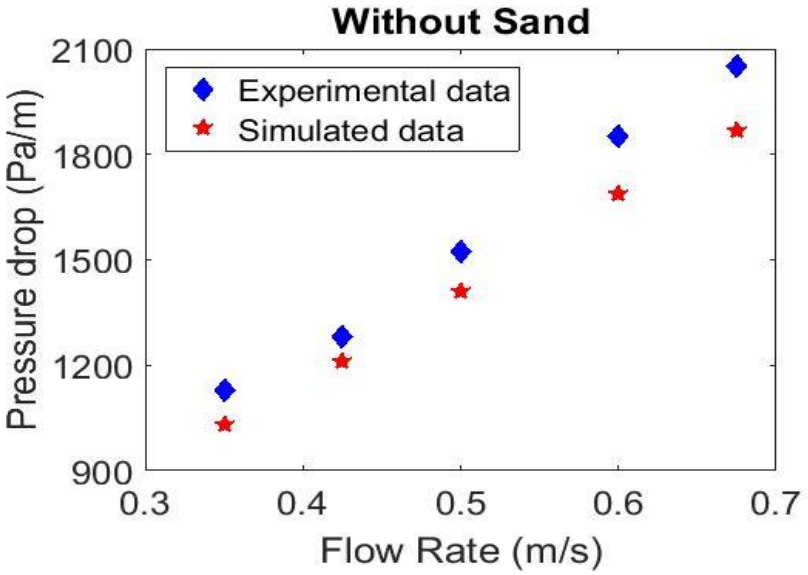

Figure 4.5: Experimental vs. simulated data without sand and without drillpipe rotation.

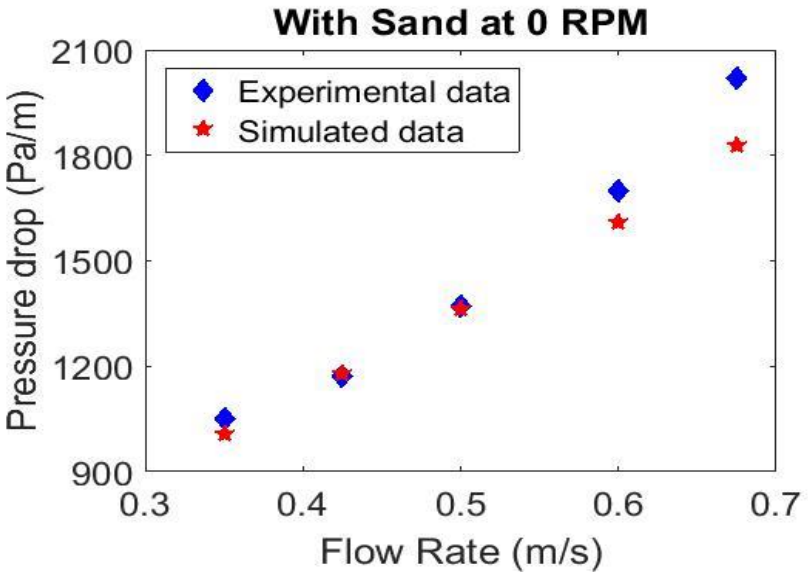

Figure 4.6: Experimental vs. simulated data with sand but without drillpipe rotation.

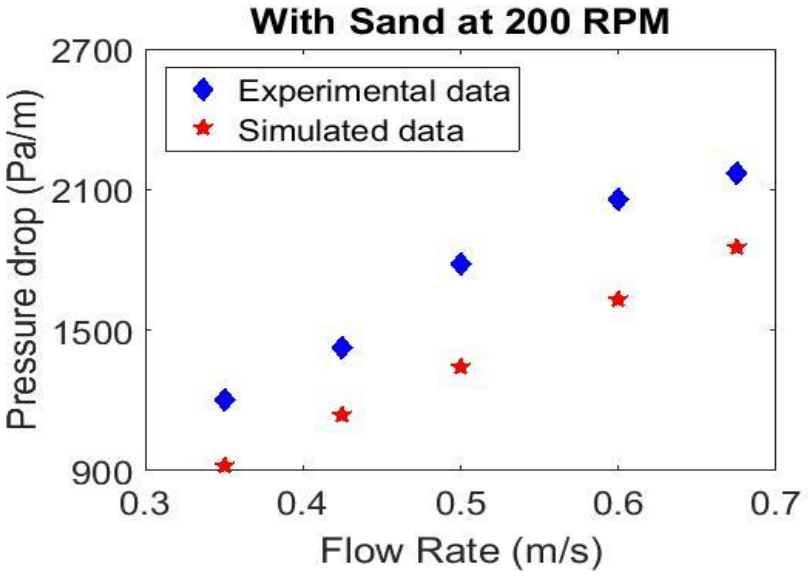

Figure 4.7: Experimental vs. simulated data with sand at 200 RPM.

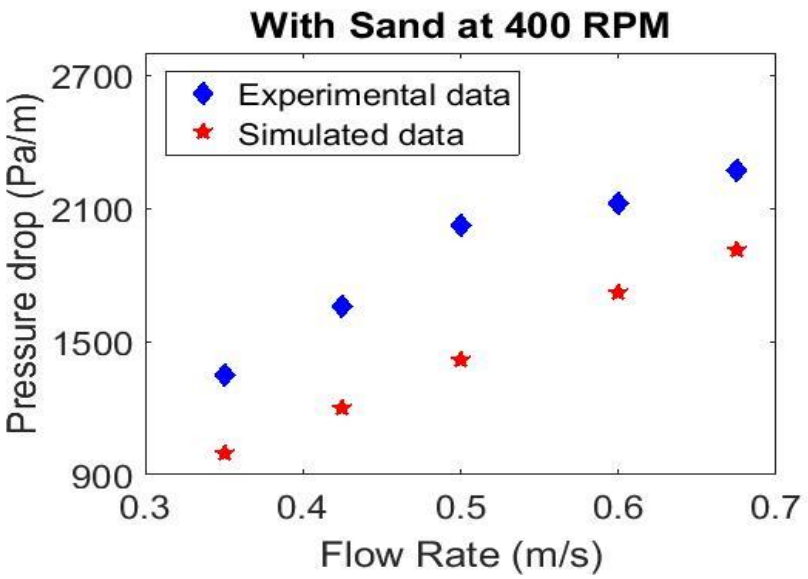

Figure 4.8: Experimental vs. simulated data with sand at 400 RPM.

Fig. 4.5 compares the experimental and simulated pressure drop without dispersed sand particles and without drillpipe rotation. The results match extremely well except the value at the highest flow rate. A possible reason for this difference is the value of the lowest viscosity used in the simulated model. Fig. 4.6 through 4.8 present the experimental and simulated pressure drop values with a feed concentration of 4% at different values of drillpipe rotation. The experimental pressure drop increase with increasing drillpipe rotation. These results do not agree with the observations made by Ahmed and Miska (2008), suggesting that the experimental setup had a slight degree of eccentricity. An increase in drillpipe rotation in an eccentric annulus causes an increase in the pressure drop values. Therefore, the underprediction of the pressure drop by the CFD model may be caused by an eccentric drillpipe.

CHAPTER 5: RESULTS AND DISCUSSION

This chapter is divided into two parts; the first part discusses the factors affecting the existence of plug zones and their effect on annular pressure drop in a viscoplastic fluid flow in a concentric vertical annulus. The second part discusses the effects of plug zones on cuttings carrying capacity of a viscoplastic fluid in a concentric vertical annulus.

5.1. Existence of Plug Zone and the Factors Affecting it

The section examines the existence and the size of plug zone in a concentric annulus with and without inner pipe rotation. The effects of various parameters on the size and growth of plug zone are considered. The fluid has been modeled using the modified bi-viscosity function. Fig. 5.1 shows plug zone as predicted by the model. It is important to mention here that all the measurements related to plug zone were made at the radial center of the annulus.

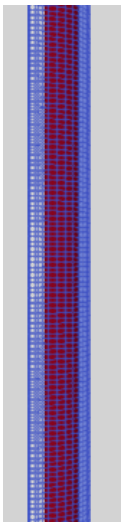

Figure 5.1: Plug zone (colored in red) in a concentric annulus

5.1.1. Effect of Yield Stress on Plug Radius

Fig. 5.2 shows the change in plug size with respect to yield stress. Plug zone is non-existent when yield stress is small. In this region, fluid does not exhibit yield. Plug zone starts to appear as yield stress increases and from this point onwards, the size of plug increases with an increase in yield stress until it reaches an upper limit. This trend has also been reported in a recently published study by Taibi and Messelmi (2017).

Simulations were rerun at different flow rates. The trend seen in Fig. 5.2 remains the same while the graph moves to the right for higher flow rates and to the left for lower flow rates. The effect of flow rate on plug size is considered in the following section.

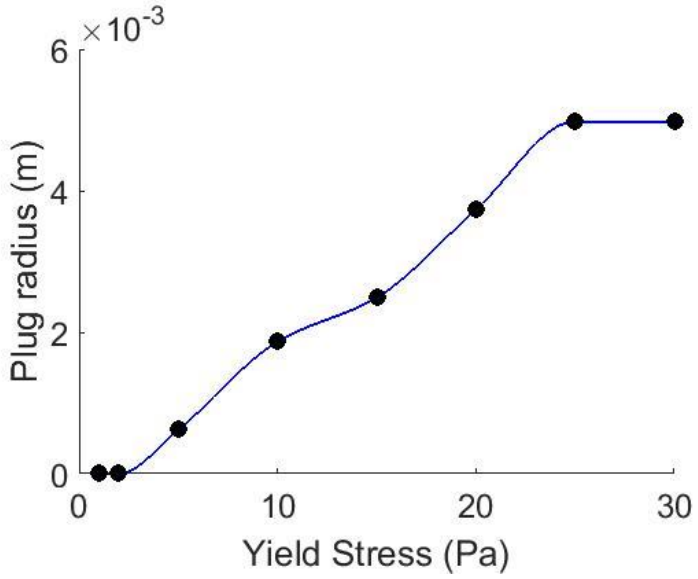

Figure 5.2: Plug zone's radius vs. yield stress

5.1.2. Effect of Flow Rate on Plug Radius

Fig. 5.3 shows the change in plug zone size with respect to flow rate. The size of plug decreases as flow rate increases until it reaches a minimum limit. The decreasing plug radius can be explained by the viscosity function. The viscosity of a viscoplastic fluid is inversely proportional to shear rate which depends on the gradient of the velocity. The modified bi-viscosity model can be written as

$$\mu = \frac{\tau_y + K|D|^n}{|D|} \quad \text{if } |D| > \frac{\tau_y}{\mu_{plug}} \tag{5.1}$$

where D is strain rate tensor and |D| is the magnitude of strain rate tensor.

Strain rate tensor, D, and its magnitude, |D|, are defined as

$$D = \frac{1}{2}(\nabla U + \nabla U^T)$$
$$|D| = [D:D]^{\frac{1}{2}} \tag{5.2}$$

where U is velocity.

An increase in velocity leads to an increase in the magnitude of strain rate tensor (eq. 5.2). It can be observed from eq. 5.1 that this increase will cause plug radius to decrease.

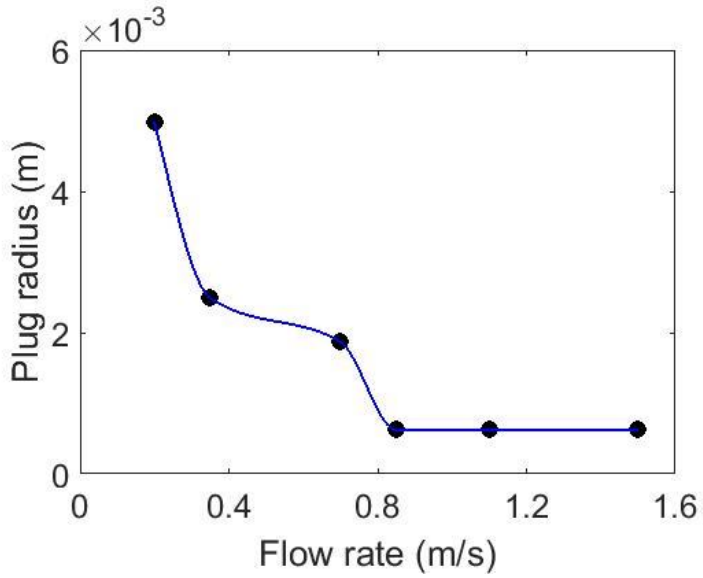

Figure 5.3: Plug zone's radius vs. flow rate

5.1.3. Effect of Annular Radius on Plug Radius

Fig. 5.4 shows the effect of annular radius on plug radius. The size of plug increases with an increase in annular radius. This increase is more significant at lower velocities which is evident from fig. 5.3. The curves for 0.75 m/s and 1 m/s are exactly same which indicates that the minimum limit observed in fig. 5.3 has been achieved.

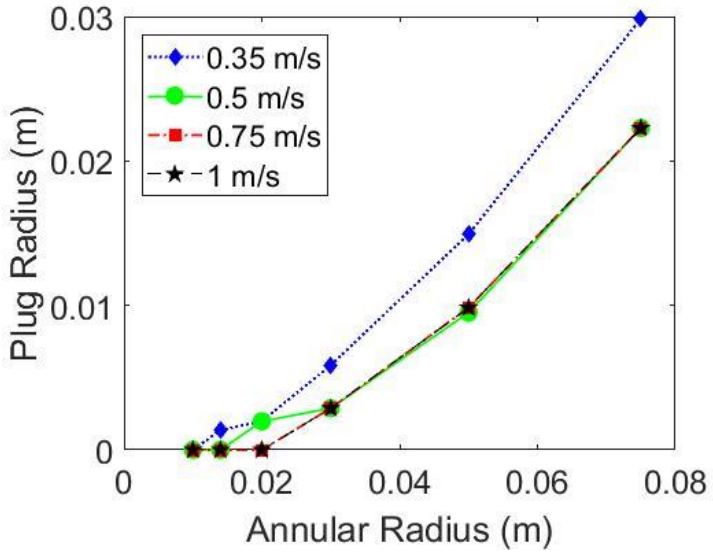

Figure 5.4: Plug zone's radius vs. annular radius

5.1.4. Plug Zones in an Eccentric Annulus

The results observed in the previous three sections can be used to predict the existence of plug zones in an eccentric annulus. Velocity profile is asymmetric in an eccentric annulus; the velocity is lower in the low side as compared to the high side. This type of non-uniform velocity profile will yield plugs of varying size throughout the eccentric annulus. The existence and growth of plug zones in a three-dimensional eccentric annulus will be the focus of author's future work.

5.1.5. Effect of Inner Pipe Rotation on Plug Size

Plug is sheared if inner pipe is rotated at a speed greater than a critical speed. Fig. 5.5 shows the effect of inner pipe rotation on plug radius at different plug viscosities. Plug is sheared at lower values of rotational speed as plug viscosity increases. This shows that the critical rotational speed is inversely proportional to plug viscosity.

Bittleston and Hassager (1992) presented an expression for Bingham Plastic fluids that predicted a critical speed of rotation of the boundary wall above which plug ceases to exist. The expression presented by Bittleston and Hassager (1992) is given as:

$$u_c = B - \frac{1}{2}B^2 \sinh^{-1}\frac{1}{2B} \tag{5.3}$$

where u_c is critical speed of rotation of the boundary wall and B is the Bingham number. The Bingham Number is defined as $B = \frac{(\tau_y)R}{(U_{mean})\mu}$ where U_{mean} = mean axial velocity and R = half radius of a pipe.

The results shown in fig. 5.5 can be explained using the above-mentioned equation for a critical speed. It can be seen from the definition of the Bingham Number and eq. 5.3 that a higher viscosity leads to a smaller Bingham number and hence a smaller critical velocity.

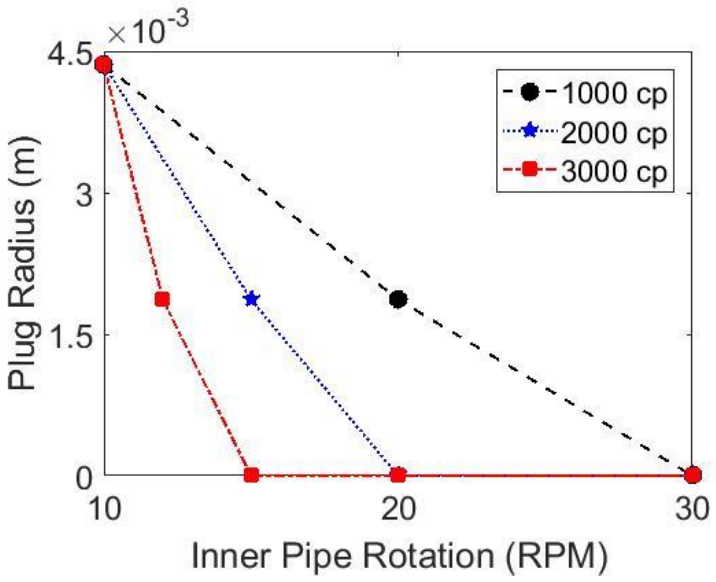

Figure 5.5: Effect of inner pipe rotation on plug zone's radius at different values of plug viscosity

Fig. 5.6 shows the effect of inner pipe rotation on plug radius at different values of yield stress. As yield stress increases, critical speed at which plug is sheared also increases showing that critical speed is directly proportional to yield stress. Again, it can be seen from the definition of the Bingham Number and eq. 5.3 that a higher value of yield stress will lead to a higher Bingham Number and hence a higher value of critical velocity.

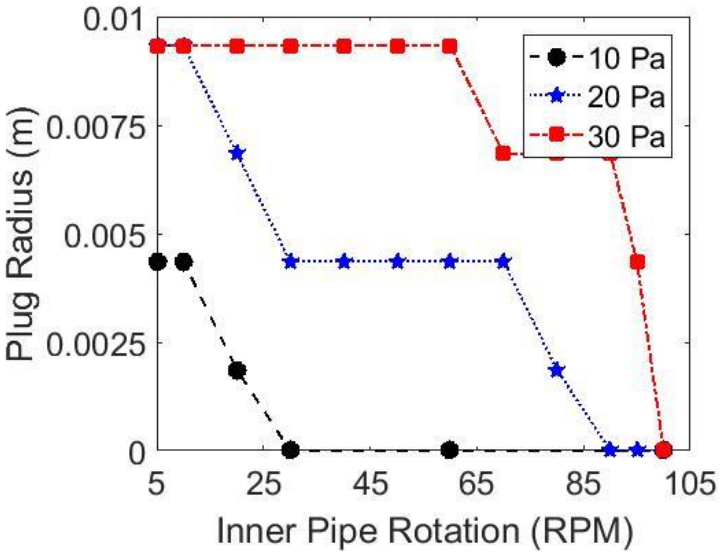

Figure 5.6: Effect of inner pipe rotation on plug zone's radius at different values of yield stress

Fig. 5.7 shows the relation between critical speed of rotation (the speed at which plug ceases to exist) and flow rate. Only speed of rotation and flow rate were varied while other parameters that included yield stress, viscosity of plug zone and wellbore geometry were kept constant. A clear trend cannot be established from fig. 5.7. It cannot be determined whether the critical speed is directly or inversely proportional to flow rate. The results suggest the critical speed is also a function of some other factor besides flow rate.

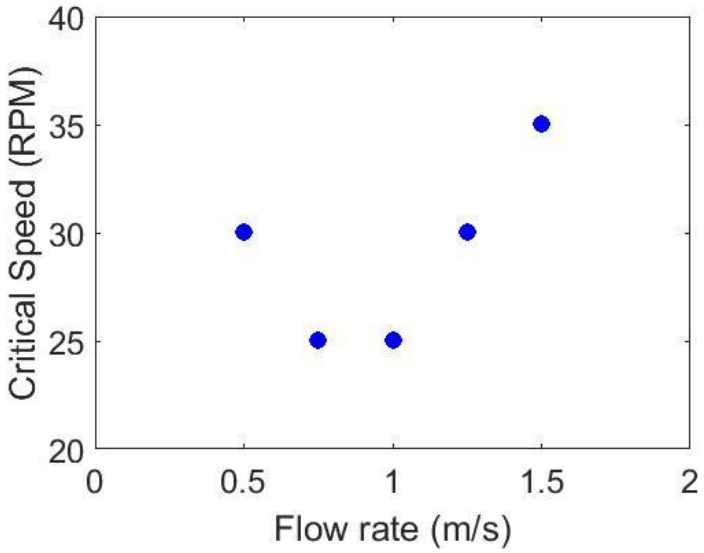

Figure 5.7: Effect of flow Rate on critical speed of rotation

5.1.6. Effect of Inner Pipe Rotation on Annular Pressure Drop

Fig. 5.8 shows the change in annular pressure drop against speed of rotation at different flow rates. Annular frictional pressure drop decreases with an increase in rotational speed. This happens because in a perfectly concentric annulus, shear thinning is the dominant flow phenomenon and the cause of reduction in pressure drop but this effect is minimal at higher flow rates. The rate of change of apparent viscosity with shear rate decreases as flow rate increases.

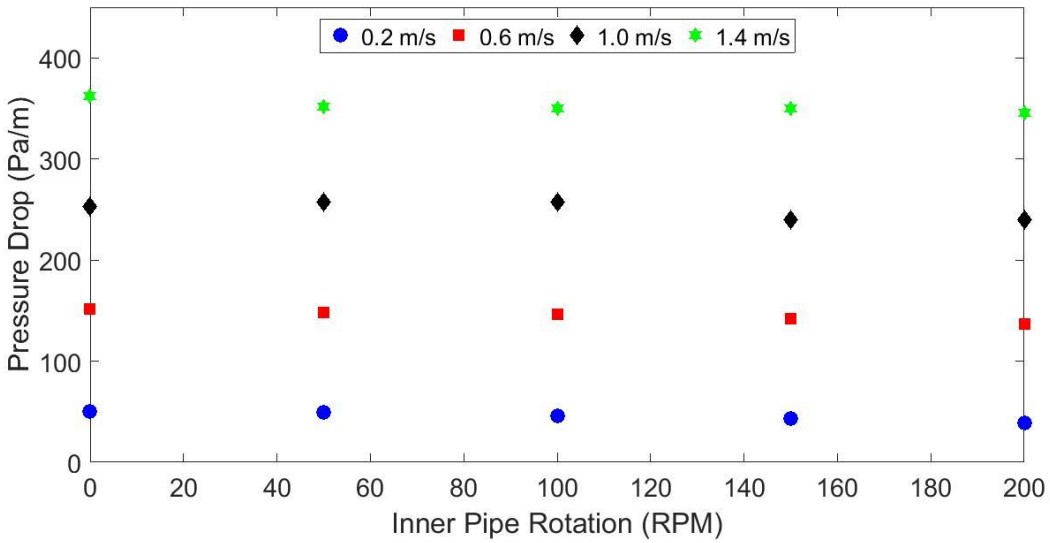

Figure 5.8: Pressure drop vs. inner pipe rotation at different flow rates

5.1.7. Effect of Plug Viscosity on Annular Pressure Drop

Fig. 5.9 shows the effect of yield stress on annular pressure drop at different flow rates. Pressure drop increases with an increase in yield strength at all values of flow rates. Fig. 5.10 shows the effect of plug viscosity on annular pressure drop. Pressure drop is found to increase with an increase in plug viscosity, but this increase is very small as compared to the increase in pressure drop with respect to yield stress. The pressure drops in an annulus primarily due to the fluid moving against the walls. The pressure drop due to fluid layers moving against each other is comparatively small. A higher viscosity plug region only affects the pressure drop due to the motion of fluid layers against each other therefore pressure drop in Fig. 5.10 is very small.

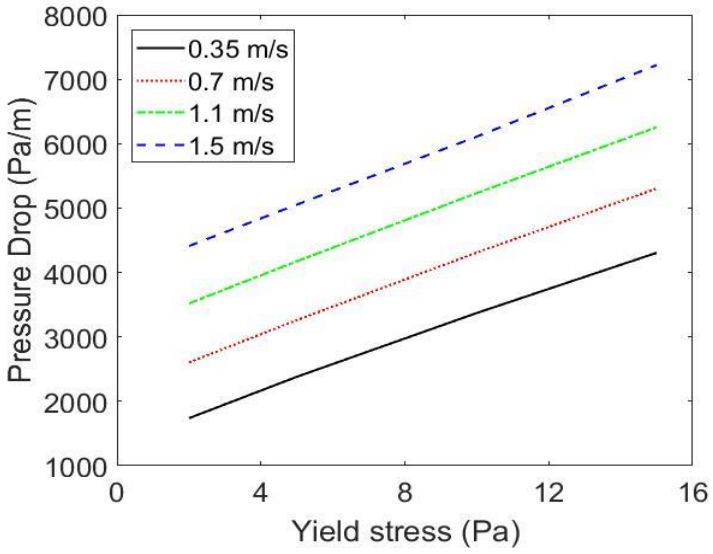

Figure 5.9: Effect of yield stress on annular pressure drop at different flow rates

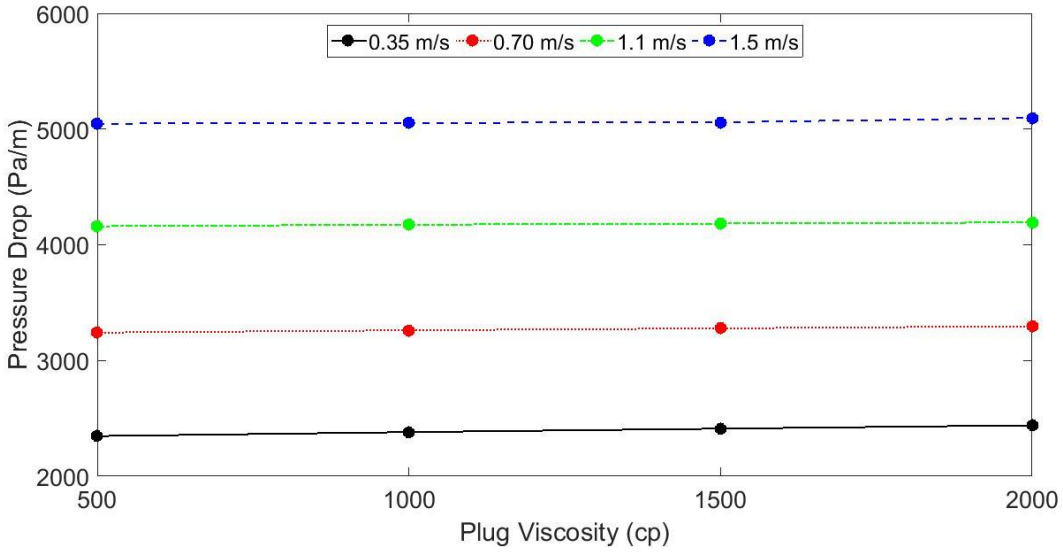

Figure 5.10: Effect of plug viscosity on annular pressure drop at different flow rates

5.2. Effect of Plug Zone on Cuttings Carrying Capacity

This part of the thesis deals with the effect of plug zone on cuttings carrying capacity of a fluid in a concentric vertical annulus. The effect of plug viscosity on cuttings concentration is investigated while varying different parameters such as cuttings size and density. Fig. 5.11 to 5.14 show the effect of different plug viscosities on cutting concentration. The parameters used for these cases are summarized in table 5.1. Flow rate was kept unchanged for all the simulations carried out in this section.

Table 5.1: Parameters used for Figures 5.11 to 5.14

	Particle Size (m)	**Particle Density (kg/m^3)**	**Annulus (m) OD x ID**	**K (Pa s)**	**n**	**Yield Stress (Pa)**
Fig. 5.11	0.002	2650	0.137 x 0.0889	0.392	0.65	
Fig. 5.12		2650	0.137 x 0.0889	0.392	0.65	1
Fig. 5.13	0.002	2650	0.2 x 0.0889	0.392	0.65	1
Fig. 5.14			0.137 x 0.0889	0.392	0.65	1
Fig. 5.15			0.137 x 0.0889	0.392	0.65	5

5.2.1. Effect of Yield Stress

Fig. 5.11 compares the change in cuttings concentration with plug viscosity at different values of yield stress which are given in Table 5.1. A trend consistent in fig. 5.11a and 5.11b is the decrease in cuttings concentration with increasing plug viscosity although this change is very small. However, cuttings concentration profile is almost identical at higher viscosities (4000 cp and 5000 cp). A major difference in cuttings profile in fig. 5.11a and 5.11b is the size of plug zone. As observed earlier in section 5.1.1, the increase in the size of plug zone is due to the increase in yield stress.

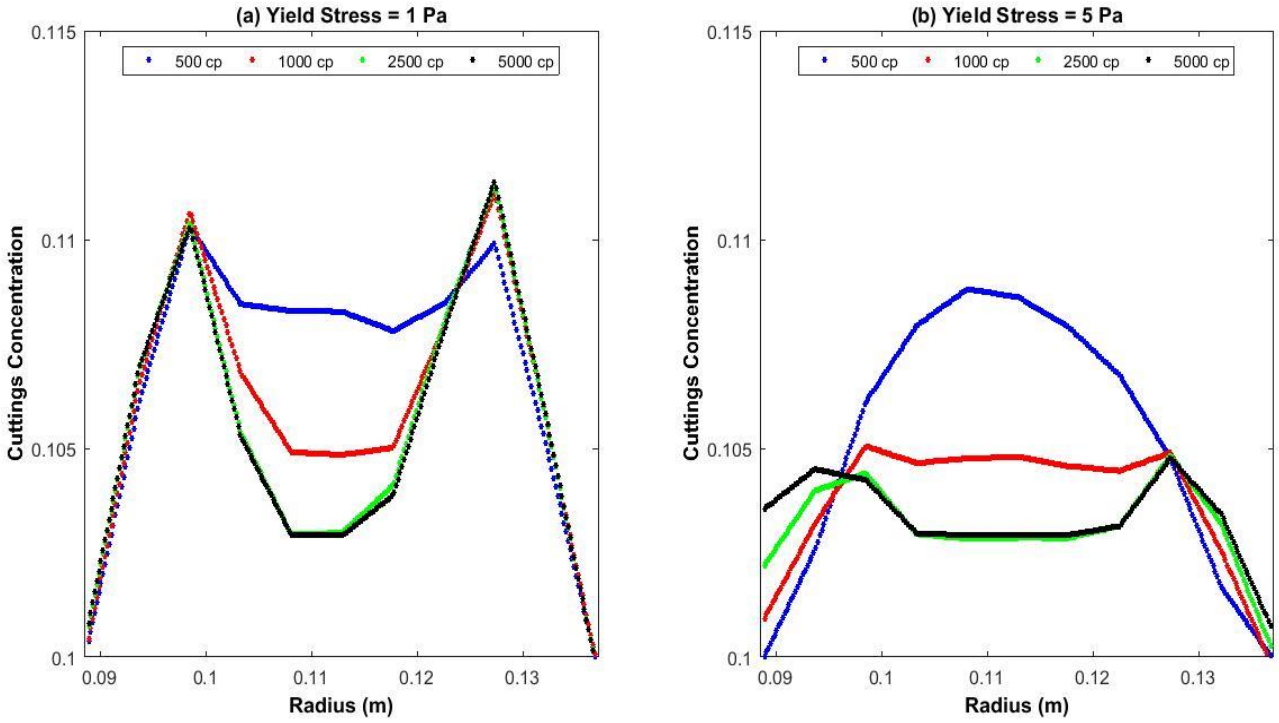

Figure 5.11: Effect of plug viscosity on cuttings concentration at different values of yield stress

5.2.2. Effect of Particle Size

Fig. 5.12 compares the change in cuttings concentration with plug viscosity at different particle sizes. The parameters used for this case are given in Table 5.1. Cuttings concentration is higher in fig. 5.12b than in fig. 5.12a. This difference is because cuttings carrying efficiency of a fluid decreases as particle size increases. In both fig. 5.12a and 5.12b, cuttings concentration decreases as plug viscosity increases but this change is very small.

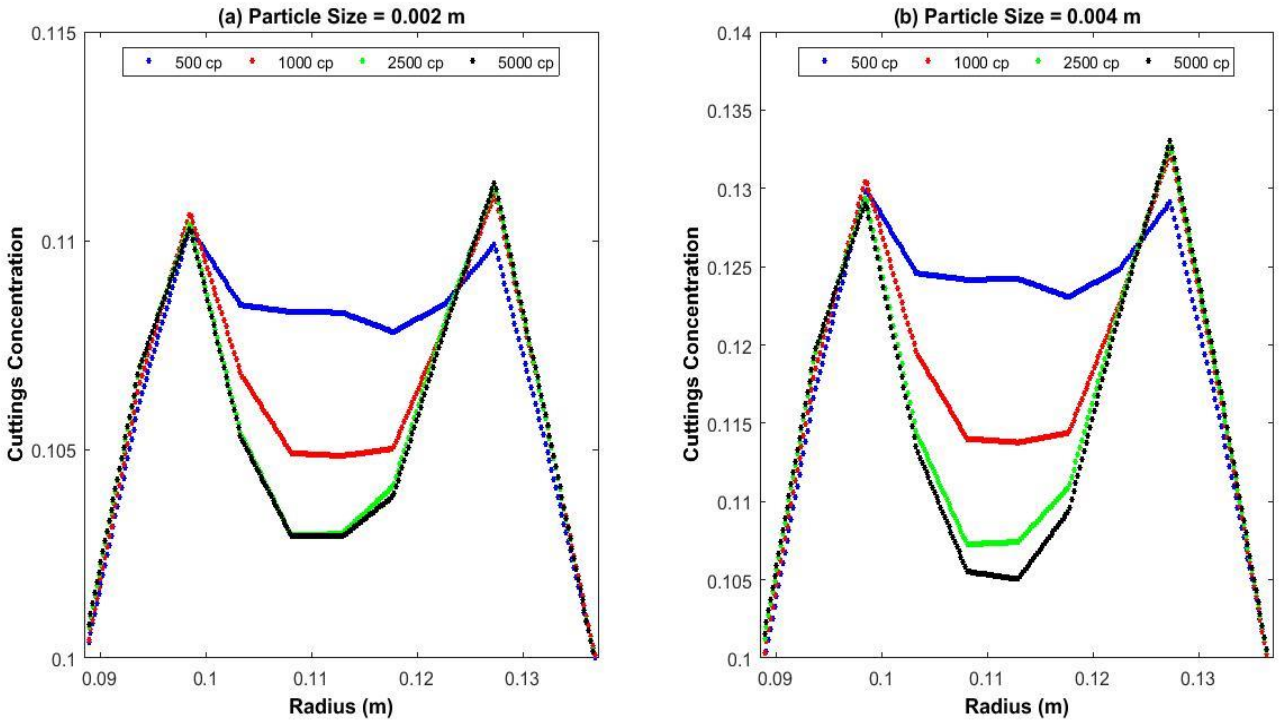

Figure 5.12 Effect of plug viscosity on cuttings concentration at different particle sizes

5.2.3. Effect of Annular Radius

Fig. 5.13 compares change in cuttings concentration with plug viscosity at different annular radii. As observed in the previous two cases, cuttings concentration decreases with increasing plug viscosity, but the change in cuttings concentration is small. The size of plug zone is greater in fig. 5.13a than in fig. 5.13b. As noted earlier in section 5.1.3, this happens because the size of plug zone increases with an increase in annular radius.

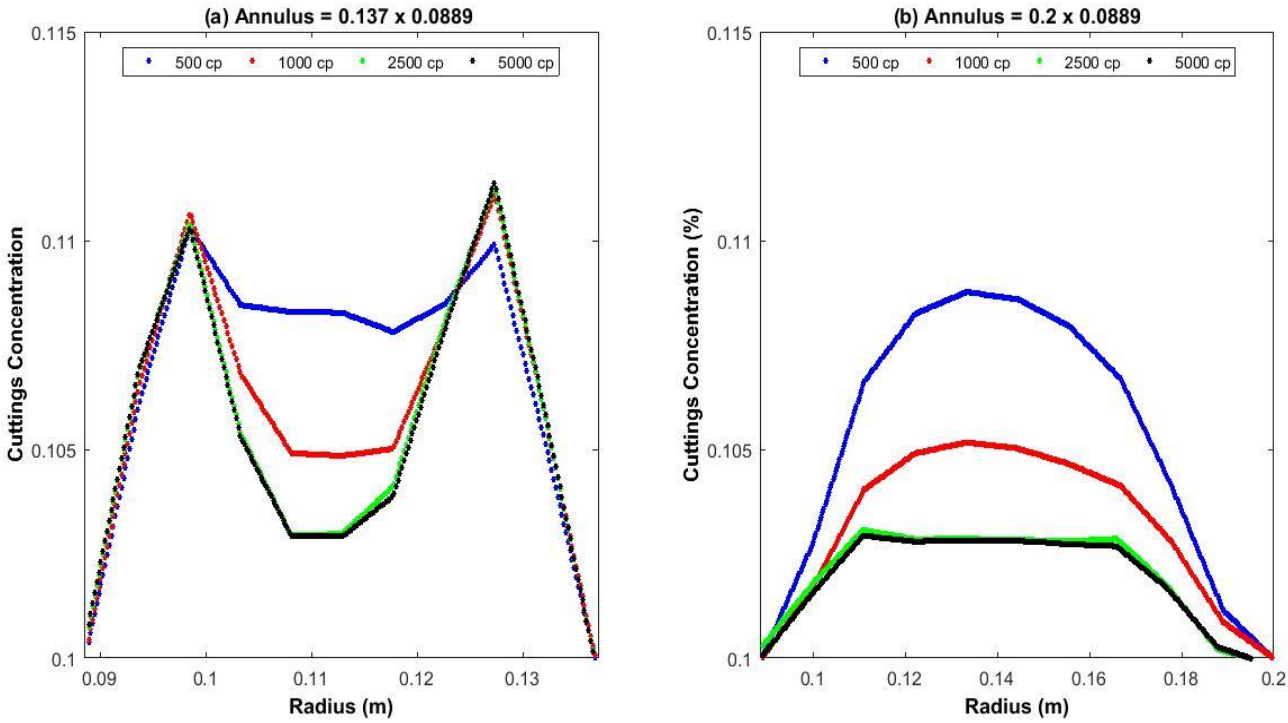

Figure 5.13: Effect of plug viscosity on cuttings concentration at different annular sizes (OD x ID)

5.2.4. Effect of Bigger and Heavier Particles

Fig. 5.14 and 5.15 compare cuttings concentration profile of a smaller and lighter particle with a bigger and heavier one. The parameters used are listed in table 5.2.1. Cuttings concentration in fig. 5.14b and 5.15b are higher than in fig. 5.14a and 5.15a because the particle is bigger and heavier. Both fig. 5.14 and 5.15 show the same trend that was observed in the previous sections. Cuttings concentration decreases with increasing plug viscosity, but the change is small.

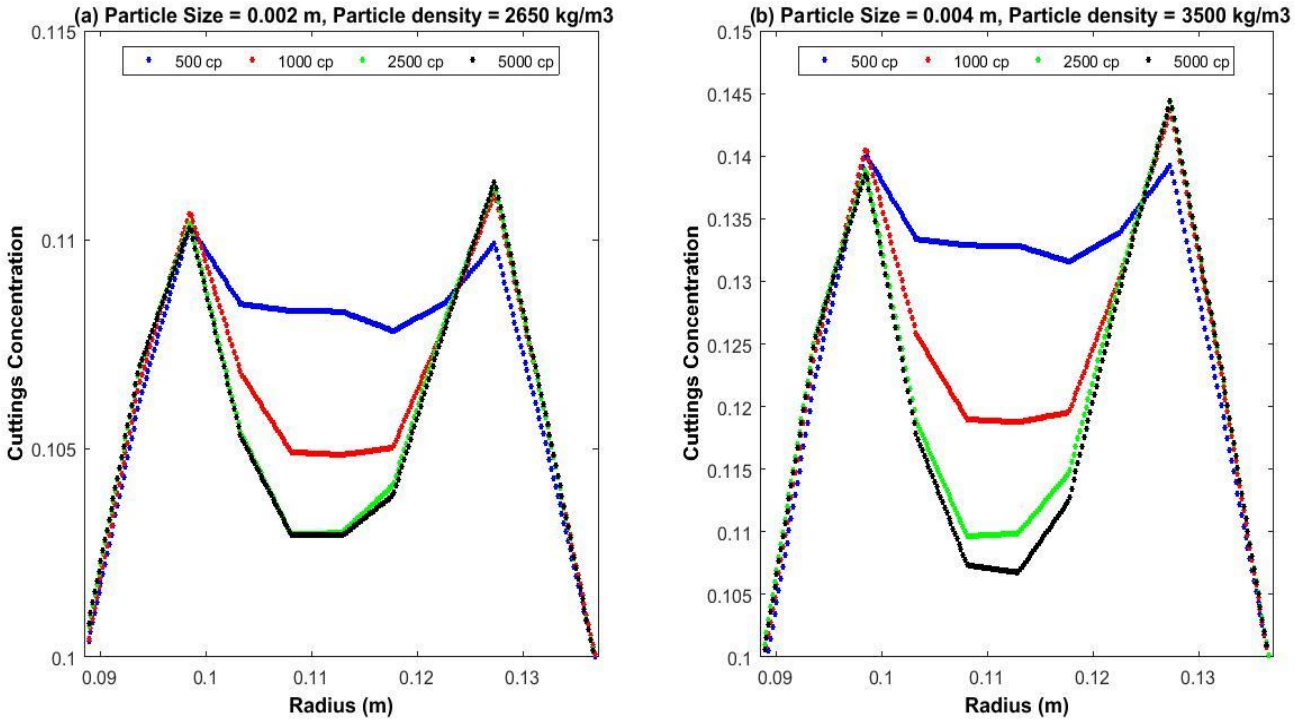

Figure 5.14: Effect of plug viscosity on cuttings concentration at particles of different sizes and densities. Yield stress is 1 Pa.

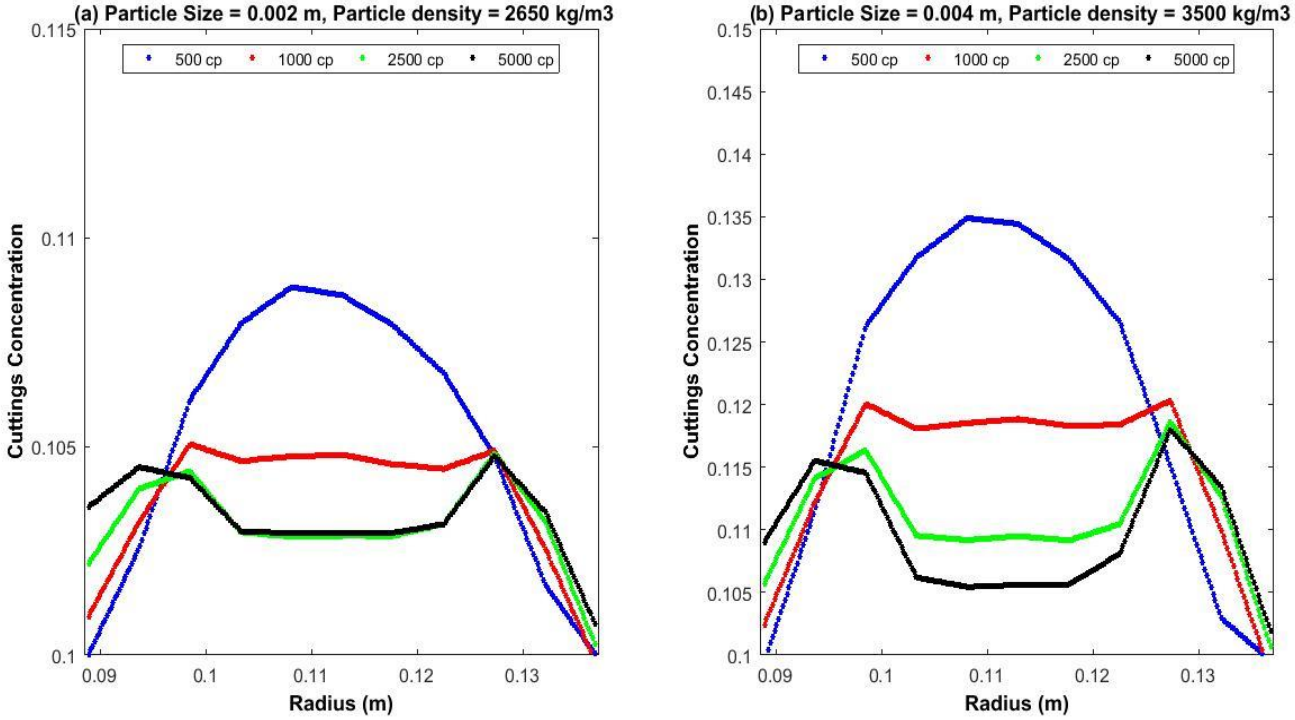

Figure 5.15: Effect of plug viscosity on cuttings concentration at particles of different sizes and densities. Yield stress is 5 Pa.

Higher values of cuttings concentration correspond to lower cutting carryings capacity of a fluid. From fig. 5.11 to 5.15, it can be concluded that cuttings carrying capacity of a fluid increases as plug viscosity increases. Though, the effect of plug viscosity on cuttings carrying capacity is very small in some cases. It can be seen from fig. 5.11 to 5.15 that the effect of plug viscosity is most significant at large particle size and/or heavy particles. These observations are in line with the consensus in the literature that the most important factor for efficient hole cleaning in a vertical well is the axial annular velocity of the fluid.

5.3. Effect of Plug Zone on Annular Pressure Drop in the Presence of Drill Cuttings

Section 5.1.7 showed that the change in the annular pressure drop in the absence of drill cuttings is very small at all values of flow rate. This section discusses the effects of different plug viscosities on annular pressure drop in the presence of drill cuttings.

Fig 5.16 shows the effect of plug viscosity on annular pressure drop in the presence of drill cuttings of different sizes. In fig. 5.16, the small particle refers to a spherical drill cutting that has a diameter of 2 mm and a density of 2650 kg/m^3. Whereas, the large particle as a diameter of 4 mm and 3500 kg/m^3. Flow rate and the initial concentration of drill cuttings were kept constant at 0.35 m/s and 4% respectively. Except the size, density and yield stress mentioned in the figure, all other parameters were kept constant.

It can be seen from fig. 5.16 that the pressure drop does not vary with plug viscosity for low values of yield stress but there is a significant change in pressure drop when yield stress is 10 Pa. At this yield stress, the rate of change of pressure drop with change in plug viscosity decreases as plug viscosity increases, pressure drop is almost constant for plug viscosities greater than 2000 cp. This trend is further investigated in fig. 5.17.

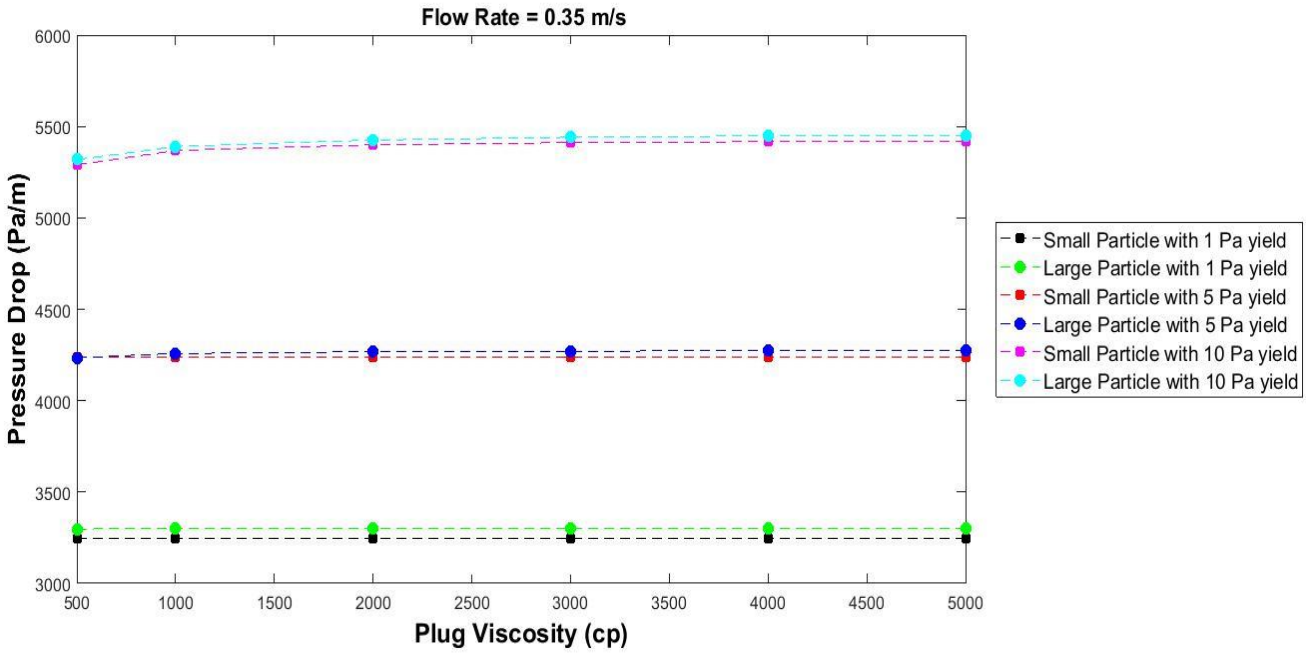

Figure 5.16: Change in annular pressure drop with plug viscosity. Flow rate = 0.35 m/s and feed cuttings concentration = 4%.

Fig. 5.17 shows the effect of plug viscosity on annular pressure drop at a flow rate of 0.10 m/s. The initial concentration, size and density of cuttings and other parameters were kept unchanged from the previous figure. When compared to the previous figure, the effect of plug viscosity is more pronounced at higher values of yield stress. As observed in the previous case, pressure drop is constant when yield stress is 1 Pa but increases significantly as yield stress increases. When compared with fig. 5.16, the change in the pressure drop is more pronounced which can be attributed to the change in flow rate.

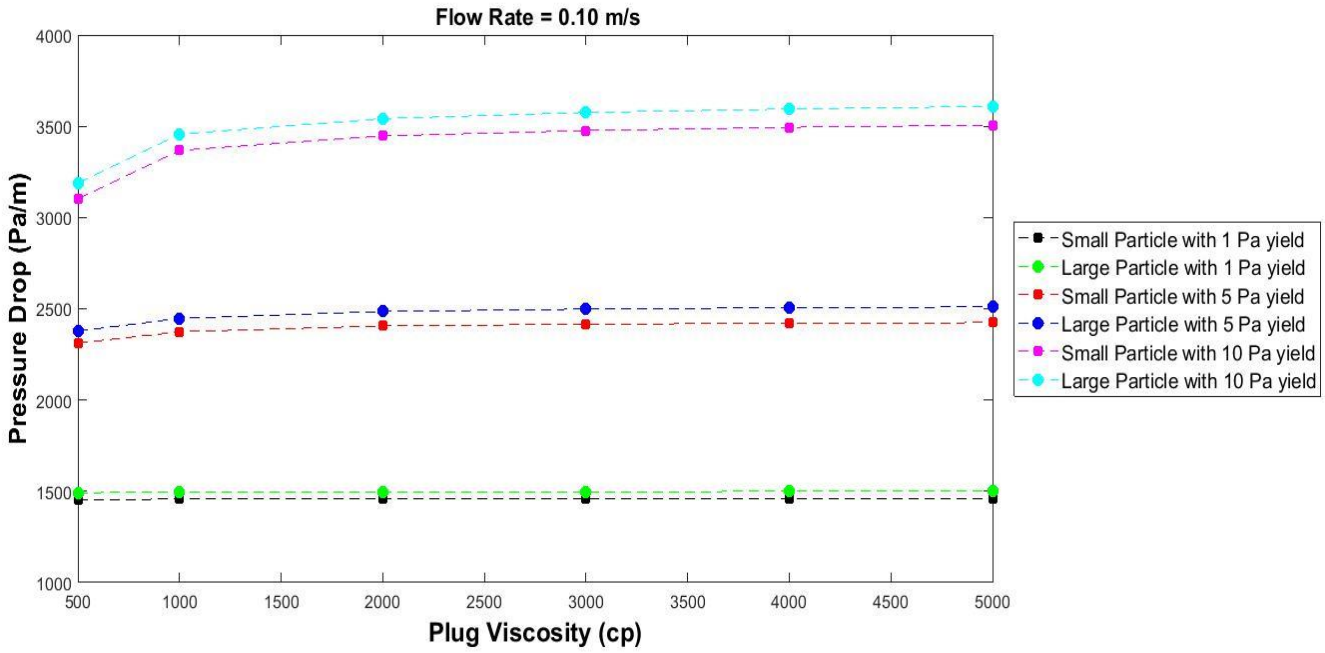

Figure 5.17: Change in annular pressure drop with plug viscosity. Flow rate = 0.10 m/s and feed cuttings concentration = 4%.

Fig. 5.18 and 5.19 show the effect of plug viscosity on annular pressure drop at 10% cuttings concentration. Only the large particles (4 mm diameter and 3500 kg/m^3) were considered for these cases. All other parameters were kept unchanged from the previous cases. The same trend that was observed in the previous figures is seen in fig. 5.18 and 5.19. For both flow rate values, there is no change in pressure drop when yield stress is low. The change in pressure drop with plug viscosity increases as yield stress increases although the rate of change in pressure drop decreases as plug viscosity increases.

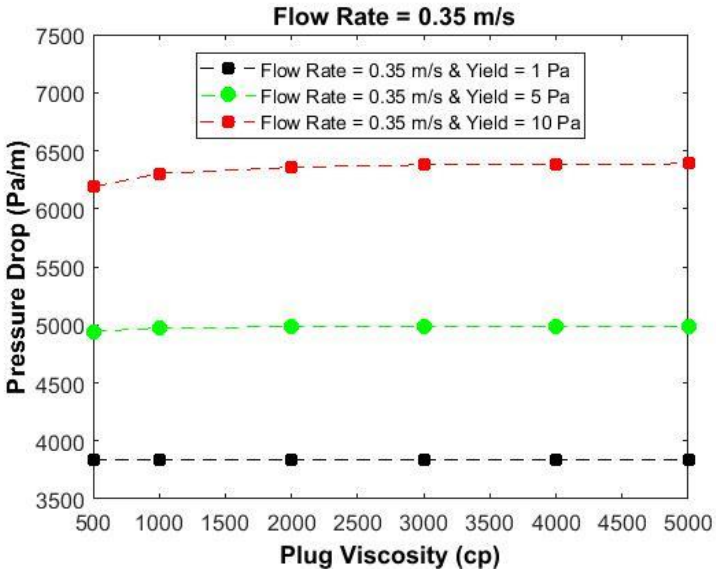

Figure 5.18: Change in annular pressure drop with plug viscosity. Flow rate = 0.35 m/s and feed cuttings concentration = 10%.

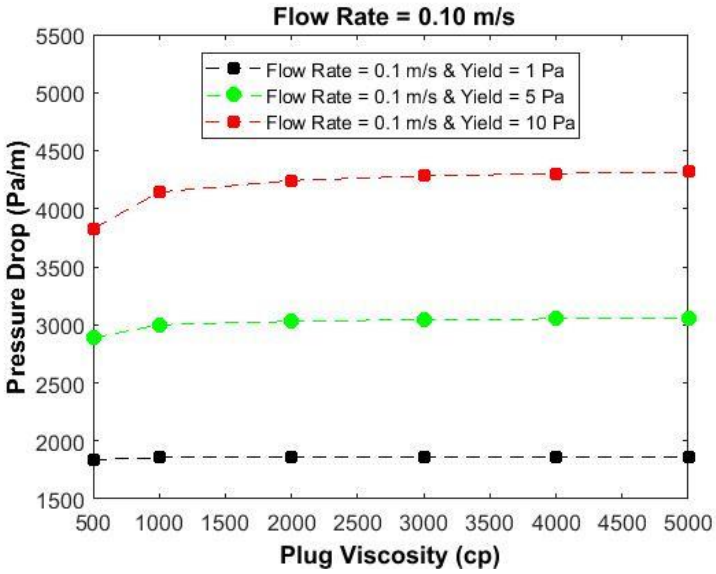

Figure 5.19: Change in annular pressure drop with plug viscosity. Flow rate = 0.10 m/s and feed cuttings concentration = 10%.

A trend consistent throughout fig. 5.16 to 5.19 is the increase in the change of pressure drop with plug viscosity as yield stress increases. As shown in section 5.1.1, the size of plug zone increases as yield stress increases. This shows that plug viscosity has a significant role at higher yield stress which corresponds to a bigger plug size. This behavior is consistent for both particle sizes suggesting that the particle size does not have a significant impact on the change in pressure drop with plug viscosity. For all the cases discussed above, the change in pressure drop is higher when plug viscosity is low but reaches a constant value above a certain viscosity value. The value of plug viscosity after which the pressure drop does not change also varies with yield stress and flow rate. At higher flow rate, the effect of plug viscosity is less significant that it is at lower flow rate. As shows in section 5.1.2, the size of plug zone decreases as flow rate increases therefore, the effect of plug zone and its viscosity also decreases as flow rate increases.

Is it an established fact in the literature that for a vertical well, flow rate plays the primary role in cuttings transport. Therefore, at high flow rates the system effectively reduces to the one studied in section 5.1.7. From the results presented above, it is concluded that at low flow rate and high yield stress, plug viscosity has a significant impact on the annular pressure drop. As flow rate increases and/or yield stress decreases, the effect of plug viscosity on annular pressure drop diminishes.

The conventional way of modeling the rheology of a drilling fluid is by using power law parameters (n and K) and yield stress value. This study shows that fluids with different plug viscosities have different effect on drilling hydraulics. Therefore, for accurate modeling of drilling hydraulics, the effect of plug zones must be considered and incorporated in the rheological models. A possible choice of the rheological model is the modified Herschel Bulkley model presented by (de Souza Mendes and Dutra, 2004) that predicts the viscosity of plug zones. The model is given as:

$$\tau = (1 - e^{-\frac{\mu_{plug}\gamma}{\tau_y}})(\tau_y + K|\gamma|^n) \quad (5.4)$$

where μ_{plug} is the viscosity of plug zone.

The results of this paper also suggest that plug zones have a greater effect on drilling hydraulics in an inclined annulus since the rheology of a fluid plays a bigger role in the inclined well than in a vertical well. This study lays the groundwork for existence of plug zones and their effect on drilling hydraulics in eccentric inclined annulus which will be the focus of author's future work.

CHAPTER 6: CONCLUSIONS AND FUTURE WORK

6.1. Conclusions

This thesis investigates the factors that affect plug zones in viscoplastic fluid flow and the impact these plug zones have on cuttings carrying capacity of a fluid and on annular pressure drop in a concentric vertical annulus. The following conclusions can be drawn from the results of this study.

- Plug zone is nonexistent when yield stress is small. The size of plug increases and reaches a maximum limit as yield stress increases.
- The size of plug zone decreases and reaches a minimum limit as flow rate increases.
- Plug is sheared if inner pipe is rotated at a speed greater than the critical speed.
- The critical speed is inversely proportional to plug viscosity and directly proportional to yield stress.
- In the absence of drill cuttings, annular pressure drop increases with an increase in yield strength and plug viscosity though the change with respect to plug viscosity is very small.
- The significance of the effect of plug zone viscosity on a fluid's cuttings carrying capacity increases as the size of the particle and/or the density of the particle increases. Therefore, a fluid with higher plug zone viscosity has better cuttings carrying capacity.
- In a concentric vertical annulus, the impact of plug zone size and viscosity on annular pressure drop increases significantly as yield stress increases and/or flow rate decreases. Therefore, for accurate prediction of annular pressure drop (and BHP), viscosity of plug zone should be considered and incorporated in the rheological models.

6.2. Future Work

This study lays the groundwork for future work on the existence of plug zones and their effect on cuttings carrying capacity and annular pressure drop in eccentric inclined annulus. The results of this thesis indicate that the impact of plug zones and therefore, their significance increases as the annulus deviates from the vertical position. Furthermore, the effect of flow rate on the critical speed of rotation needs more investigation.

References

Adekomaya, O., Olafuyi, O., others, 2011. An Experimental Study of the Effect of Contaminants on the Flow Properties of Oil based Drilling Mud. Pet. Coal 53.

Ahmed, R.M., Miska, S.Z., 2008. Experimental Study and Modeling of Yield Power-Law Fluid Flow in Annuli With Drillpipe Rotation, in: IADC/SPE Drilling Conference. Society of Petroleum Engineers.

Al-Kayiem, H.H., Ismail, M., Zaki, N., Elfeel, M.E., 2010. Simulation of the cuttings cleaning during the drilling operation. Am. J. Appl. Sci. 7, 800–806.

Astarita, G., 1990. Letter to the Editor: The engineering reality of the yield stress. J. Rheol. 34, 275–277.

Barnes, H.A., Walters, K., 1985. The yield stress myth? Rheol. Acta 24, 323–326.

Beris, A., Tsamopoulos, J., Armstrong, R., Brown, R., 1985. Creeping motion of a sphere through a Bingham plastic. J. Fluid Mech. 158, 219–244.

Beverly, C., Tanner, R., 1992. Numerical analysis of three-dimensional Bingham plastic flow. J. Non-Newton. Fluid Mech. 42, 85–115.

Beverly, C.R., Tanner, R.I., 1989. Numerical Analysis of Extrudate Swell in Viscoelastic Materials with Yield Stress. J. Rheol. 33, 989–1009.

Bingham, E.C., 1922. Fluidity and plasticity. McGraw-Hill, New York.

Bird, R.B., Dai, G., Yarusso, B.J., 1983. The rheology and flow of viscoplastic materials. Rev. Chem. Eng. 1, 1–70.

Bittleston, S.H., Hassager, O., 1992. Flow of viscoplastic fluids in a rotating concentric annulus. J. Non-Newton. Fluid Mech. 42, 19–36.

Buscall, R., Goodwin, J., Ottewill, R., Tadros, T.F., 1982. The settling of particles through Newtonian and non-Newtonian media. J. Colloid Interface Sci. 85, 78–86.

Casson, N., 1959. Rheology of disperse systems. Ed CC Mill Pergamon Press Oxf.

Clark, R., Bickham, K., 1994. A mechanistic model for cuttings transport, in: SPE Annual Technical Conference and Exhibition. Society of Petroleum Engineers.

de Souza Mendes, P.R., Dutra, E.S., 2004. A viscosity function for viscoplastic liquids. Trans Nord. Rheo Soc 12, 183–188.

de Souza Mendes, P.R., Naccache, M.F., Varges, P.R., Marchesini, F.H., 2007. Flow of viscoplastic liquids through axisymmetric expansions–contractions. J. Non-Newton. Fluid Mech. 142, 207–217.

Frigaard, I.A., Nouar, C., 2005. On the usage of viscosity regularisation methods for visco-plastic fluid flow computation. J. Non-Newton. Fluid Mech. 127, 1–26.

Gavignet, A., Wick, C., 1987. Computer Processing Improves Hydraulics Optimization with New Methods. SPE Drill. Eng. 2, 309–315.

Han, S.-M., Hwang, Y.-K., Woo, N.-S., Kim, Y.-J., 2010. Solid–liquid hydrodynamics in a slim hole drilling annulus. J. Pet. Sci. Eng. 70, 308–319.

Hartnett, J.P., Hu, R.Y.Z., 1989. Technical note: The yield stress—An engineering reality. J. Rheol. 33, 671–679.

Herschel, W.H., Bulkley, R., 1926. Konsistenzmessungen von Gummi-Benzollosungen 39, 291.

Hirsch, C. (Ed.), 1988. Numerical Computation of Internal &Amp; External Flows: Fundamentals of Numerical Discretization. John Wiley & Sons, Inc., New York, NY, USA.

Hussaini, S.M., Azar, J.J., 1983. Experimental study of drilled cuttings transport using common drilling muds. Soc. Pet. Eng. J. 23, 11–20.

Ishii, M., Mishima, K., 1984. Two-fluid model and hydrodynamic constitutive relations. Nucl. Eng. Des. 82, 107–126.

Ishii, M., Zuber, N., 1979. Drag coefficient and relative velocity in bubbly, droplet or particulate flows. AIChE J. 25, 843–855.

Khalil, M., Mohamed Jan, B., 2012. Viscoplastic Modeling of a Novel Lightweight Biopolymer Drilling Fluid for Underbalanced Drilling. Ind. Eng. Chem. Res. 51, 4056–4068.

Liu, B.T., Muller, S.J., Denn, M.M., 2002. Convergence of a regularization method for creeping flow of a Bingham material about a rigid sphere. J. Non-Newton. Fluid Mech. 102, 179–191.

Manninen, M., Taivassalo, V., Kallio, S., 1998. On the mixture model for multiphase flow 67.

Mohammadzadeh, K., Hashemabadi, S., Akbari, S., 2016. CFD simulation of viscosity modifier effect on cutting transport by oil based drilling fluid in wellbore. J. Nat. Gas Sci. Eng. 29, 355–364.

O'Donovan, E.J., Tanner, R.I., 1984. Numerical study of the Bingham squeeze film problem. J. Non-Newton. Fluid Mech. 15, 75–83.

Ofei, T., Irawan, S., Pao, W., 2015. Cuttings-liquid frictional pressure loss model for horizontal narrow annular flow with rotating drillpipe, in: IOP Conference Series: Materials Science and Engineering. IOP Publishing, p. 012009.

Ostwald, W., De Waele, A., 1923. Oil and color. Chem Assoc J 6, 23–24.

Özbelge, T.A., Beyaz, A., 2001. Dilute solid–liquid upward flows through a vertical annulus in a closed loop system. Int. J. Multiph. Flow 27, 737–752.

Papanastasiou, T.C., 1987. Flows of Materials with Yield. J. Rheol. 31, 385–404.

Robertson, R., Stiff Jr, H., others, 1976. An improved mathematical model for relating shear stress to shear rate in drilling fluids and cement slurries. Soc. Pet. Eng. J. 16, 31–36.

Schiller, L., Naumann, A., 1935. A Drag Coefficient Correlation. Z. Ver. Dtsch. Ingenieure 77, 318–320.

Schurz, J., 1990. The yield stress ? An empirical reality. Rheol. Acta 29, 170–171.

Sifferman, T.R., Myers, G.M., Haden, E.L., Wahl, H.A., others, 1974. Drill cutting transport in full scale vertical annuli. J. Pet. Technol. 26, 1–295.

Sisko, A., 1958. The flow of lubricating greases. Ind. Eng. Chem. 50, 1789–1792.

Taibi, H., Messelmi, F., 2017. Effect of yield stress on the behavior of rigid zones during the laminar flow of Herschel-Bulkley fluid. Alex. Eng. J.

Tanner, R., Milthorpe, J., 1983. Numerical simulation of the flow of fluids with yield stress, in: Proc. 3rd Int. Conf., Seattle, Pineridge Press, Swansea. pp. 680–690.

Ungarish, M., 1993. Hydrodynamics of Suspensions: Fundamentals of Centrifugal and Gravity Separation. Springer-Verlag, Berlin Heidelberg.

Verloop, W., 1995. The inertial coupling force. Int. J. Multiph. Flow 5, 929–933.

Wildemuth, C.R., Williams, M.C., 1985. A new interpretation of viscosity and yield stress in dense slurries: Coal and other irregular particles. Rheol. Acta 24, 75–91.